AD-A037 736 PERSON (LEIF N) TRONDHEIM (NORWAY) F/G 20/11
EXPERIMENTAL STUDY OF A TUNNEL'S COLLAPSE CRITERION.(U)
JAN 77 L N PERSEN F44620-75-C-0029

UNCLASSIFIED AFGL-TR-77-0069 NL

| QF |
AD
A037736

END

DATE
FILMED
4-77

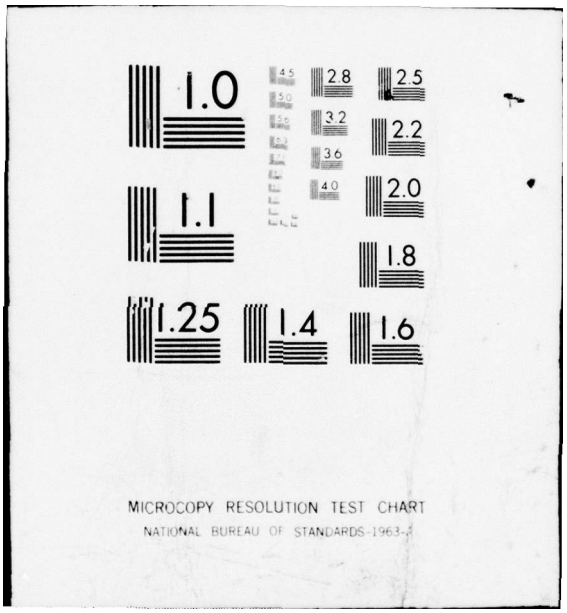
1.0
1.1
1.25
1.4
1.6
1.8
2.0
2.2
2.5
2.8
3.2
3.6
4.0
4.5
5.0
MICROCOPY RESOLUTION TEST CHART
NATIONAL BUREAU OF STANDARDS-1963-A

AFGL-TR-77-0069

EXPERIMENTAL STUDY OF A TUNNEL'S COLLAPSE CRITERION

Leif N. Persen

Institute of Applied Mechanics
University of Trondheim, NTH, 7034
Trondheim, Norway

Scientific Report No. 1

31 January 1977

Approved for public release; distribution unlimited

AIR FORCE GEOPHYSICS LABORATORY
AIR FORCE SYSTEMS COMMAND
UNITED STATES AIR FORCE
HANSCOM AFB, MASSACHUSETTS 01731

Unclassified

SECURITY CLASSIFICATION OF THIS PAGE *(When Data Entered)*

REPORT DOCUMENTATION PAGE	READ INSTRUCTIONS BEFORE COMPLETING FORM
1. REPORT NUMBER: AFGL-TR-77-0069	2. GOVT ACCESSION NO.
3. RECIPIENT'S CATALOG NUMBER	
4. TITLE *(and Subtitle)*: EXPERIMENTAL STUDY OF A TUNNEL'S COLLAPSE CRITERION.	5. TYPE OF REPORT & PERIOD COVERED: Scientific Report, No. 1
	6. PERFORMING ORG. REPORT NUMBER
7. AUTHOR(s): Leif N. Persen, Professor, Institute of Applied Mechanics, University of Trondheim, NTH, 7034 Trondheim	8. CONTRACT OR GRANT NUMBER(s): F44620-75-C-0029
9. PERFORMING ORGANIZATION NAME AND ADDRESS: Leif N. Persen, Oscar Wistings vei 20B, 7000 Trondheim, Norway	10. PROGRAM ELEMENT, PROJECT, TASK AREA & WORK UNIT NUMBERS: 76391301
11. CONTROLLING OFFICE NAME AND ADDRESS: European Office of Aerospace Research and Development, (AFSC), 223/231 Old Marylebone Road London NW 1 5th, England	12. REPORT DATE: 77 Jan 31
	13. NUMBER OF PAGES: 41
14. MONITORING AGENCY NAME & ADDRESS *(if different from Controlling Office)*: Air Force Geophysics Laboratory(LWW) Hanscom AFB, Massachusetts 01731. Monitor/Ker Thomson/LWW	15. SECURITY CLASS. *(of this report)*: Unclassified
	15a. DECLASSIFICATION/DOWNGRADING SCHEDULE

16. DISTRIBUTION STATEMENT *(of this Report)*

Approved for public release; distribution unlimited

31 Jan 77

42p.

17. DISTRIBUTION STATEMENT *(of the abstract entered in Block 20, if different from Report)*

18. SUPPLEMENTARY NOTES: The present report appears as a supplement to and an integral part of the Final Report: THE APPLICATION OF THEORETICAL RESULTS IN THE DESIGN OF SAFE SHELTERS IN ROCK by Leif N. Persen

19. KEY WORDS *(Continue on reverse side if necessary and identify by block number)*

Wave propagation in rock, Shock wave/Tunnel interaction.

20. ABSTRACT *(Continue on reverse side if necessary and identify by block number)*

A review is given of the research efforts sponsored by the German Defense Ministry to investigate the early-time interaction between a shock wave and a tunnel and the subsequent collapse of the latter. The result is given in the form of empirical equations describing the motion of the wall and a suggested way of studying the collapse mechanism.

DD FORM 1 JAN 73 1473 EDITION OF 1 NOV 65 IS OBSOLETE

388 849

Unclassified

SECURITY CLASSIFICATION OF THIS PAGE *(When Data Entered)*

CONTENTS

Experimental Study of a Tunnel's Collapse Criterion

by
Leif N. Persen

Introduction.

This presentation is an attempt to gather the information obtained through experimental investigations of what in general terms might be called a cavity's "collapse criterion" as far as dynamic loading is concerned. The experiments to be considered are the ones sponsored by the Bundesministerium der Verteidigung, West Germany and carried out by A/S NORCONSULT, Oslo, Norway in the period 1968-74.

It should be emphasized right from the beginning, that the collapse criterion in the sense used here is not a single-valued physical quantity even for a given tunnel in a specific rock. A tunnel may have several "collapse criteriae" according to the definition of what should be considered "a collapse". The purpose of the tunnel will here be one of the many factors to be considered. A tunnel may serve such a purpose that it will continue to function until a more or less complete cave-in occurs. On the other hand its purpose may be to protect highly sensitive objects from shocks caused by oncoming stress waves, in which case its protective function may cease long before the tunnel as such is endangered. The collapse criterion is thus here closely linked to the cessation of the tunnel's functioning according to its purpose.

The very wide definition given above and the almost infinite variety of possible situations which may occur made it necessary to limit the scope of the investigation to a few situations of practical importance. First a distinction was made between the lined and the unlined ("raw") tunnel. Then only a certain class of linings were picked to be tested. Finally limitations were put upon the ratio between the tunnel diameter and the length of the oncoming stress wave. Within this rather restricted framework only limited information on the interaction between the tunnel and the stress wave was sought.

1. The "raw" tunnel.

The ability of a "raw" tunnel to withstand the influence of an oncoming shock wave without being damaged, depends on several conditions which may be of a rather vague character. One such condition will be the way in which the tunnel was originally excavated. As indicated in

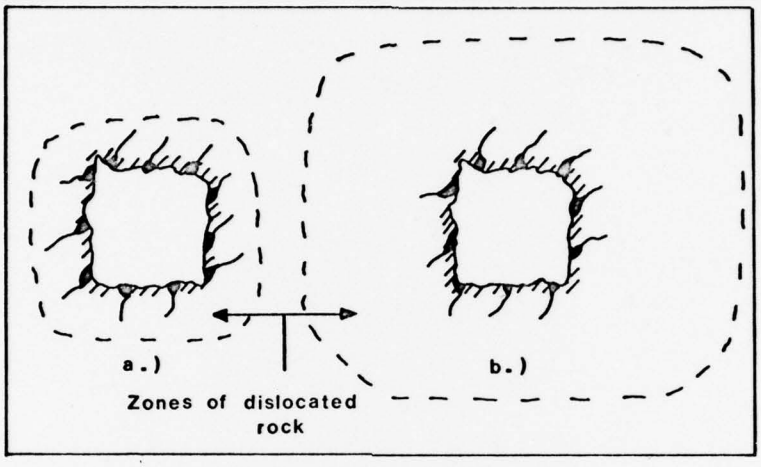

Fig.1 Dislocation zones around two similar tunnels under different conditions.

Fig.1 the dimensions of the zones of dislocated rock material around the tunnel may vary considerably depending upon the method of blasting used to excavate it as well as upon the original condition of the rock before excavation.

Another such condition will be the extent to which static stresses are present in the rock material adjacent to the tunnel. These static stresses may change with time, and even though these changes may be small and very slow, the stage may be reached at which the tunnel may collapse without any additional dynamic loading.

These two conditions show how difficult it will be to establish valid "collapse criteriae" for "raw" tunnels. They also illustrate the difficulties involved in a theoretical approach to the problem because such qualities as "degree of dislocation" is not easily quantisized as part of a description of the situation around the tunnel.

The experimental approach to the problem consisted of an attempt to perform an experiment which, when executed on location, might give an idea of the collapse criterion of a given tunnel. The idea was to excavate a test tunnel using the same procedure as that used when the

real tunnel was excavated. Because one operates on location one might hope to have the same static stresses as those present in the real tunnel neglecting the long term rearrangement which the stress at the real tunnel may have undergone. Because of the way in which the test tunnel is excavated one might also hope to have dislocation zones which are similar in the two cases. The test tunnel will preferably be made smaller than the real tunnel, and consequently the question of a model law will arise.

The idea behind the tests was to create an inward moving concentric shock wave around a circular cylindrical tunnel. One could thereby hope to take advantage of the focusing effect of the shock wave [1] so that one could create large enough stresses for impending "collapse" at the test tunnel without endangering the real tunnels in the neighborhood. This idea led to an experimental set-up illustrated in Figs.2 and 3. A circular tunnel was excavated with a vertical axis. The radius of the tunnel was $R_3 = 0.70$ [m]. On a concentric circle of radius $R_4 = 1.70$ [m] holes for pick-ups based on strain gauges were drilled. By means of these pick-ups the inward moving stress wave can be monitored. Holes for the charges were drilled on circles with radiae $R_1 = 3.10$ [m] and $R_2 = 2.40$ [m]. Cylindrical charges were used as illustrated in Fig.3 . On the walls of the tunnel were mounted accelerometers in the region where the shock wave was expected to be "plane". Fig.2 shows the real location of the charges, the pick-ups and the accelerometers in the experiment. A similar experi-

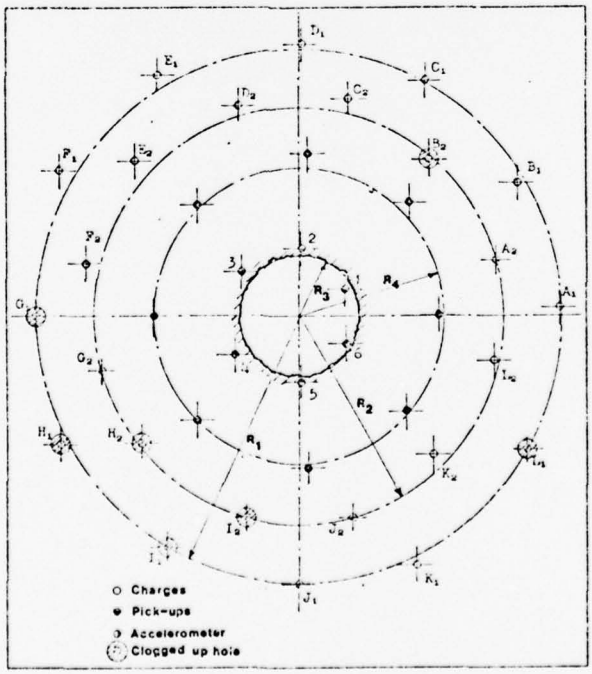

Fig. 2 Geometry of the experiment (top view)

ment was also made to see if the focusing effect of the shock wave was achieved. In that case the geometry shown in Fig.2 was kept, the tunnel was however not excavated but the accelerometers were replaced by ordinary strain gauge pick-ups placed in holes at the same location.

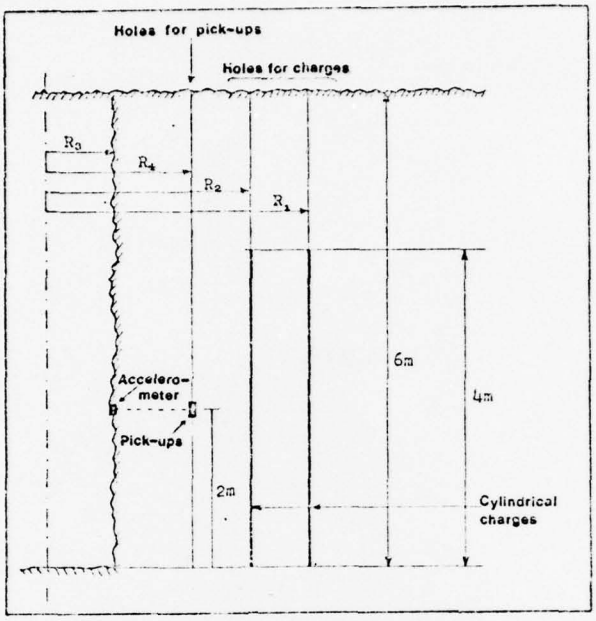

Fig.3 Geometry of the experiment (side view)

The result of these tests can be summed up as follows:

1. As could be expected, the stress waves from each source did not merge into one single nice concentric shock wave. Analysis of the the shock wave showed that it would always have to be considered as the sum of the cylindrical charges superimposed on each other. This was however sufficient for the purpose.

2. The focusing effect of the geometry was counteracted by the attenuation in such a way that the peak value of the shock wave remained constant as it moved inward. This was considered satisfactory.

3. The collapse criterion was to be determined as that value of the oncoming shock wave for which spalling of the walls started to occur. The charges were steadily increased and it turned out that no definite value could be found below which spalling did not occur. A certain amount of spalling could be traced even at very low levels. Thus it was decided to use the mass of the spall as a measure for "collapse", and a limiting value of 360 [atm] for the permissible peak value of the oncoming shock wave was finally established as the "collapse criterion" for this particular tunnel in that particular rock.

4. One would have to take account of the fact, that by steadily increasing the charges, the repeated detonations may alter the rock's properties as a wave transmitting medium.

5. The walls of the tunnel were painted in a color contrasting that of the rock so that the places where spalling had occurred could be easily found. In this way the mounted picture of the wall after the event shown in Fig.4 was obtained.

Fig.4 A mount of single photos of the tunnel walls after spalling. Dark areas indicate places where spalling has occurred.

The results obtained in these experiments needed additional support, and supplementing experiments were made in an entirely different type of rock. One of the contentions to be tested was among others the assumed geat influence on the criterion of the method used to excavate the tunnel. Two of the test tunnels were therefore drilled, leaving the neighboring rock as good as untouched, whereas the other two were excavated by cautious blasting. The geometry of the experiment is illustrated in Figs.5,6 and 7. The test tunnels I, II, III and IV extend from the four walls of the chamber A in Fig.5 . The tunnels have a radius $R_1 = 0.7$ [m] as indicated in Fig.6 . On concentric circles were drilled holes for the pick-ups (A1 - A8), and for the charges (B1 - B16). On the tunnel walls were mounted accelerometers (C1 - C6). The length of the charges were *4 m* as shown in Fig.7 where also the relative postion of the pick-ups and the accelerometers is shown.

The charges were increased in steps until spalling took place to such an extent that the tunnel was considered useless as shelter. The value of the maximum amplitude of the shock wave for which this occurred was taken as the collapse criterion. It is however clear that this value

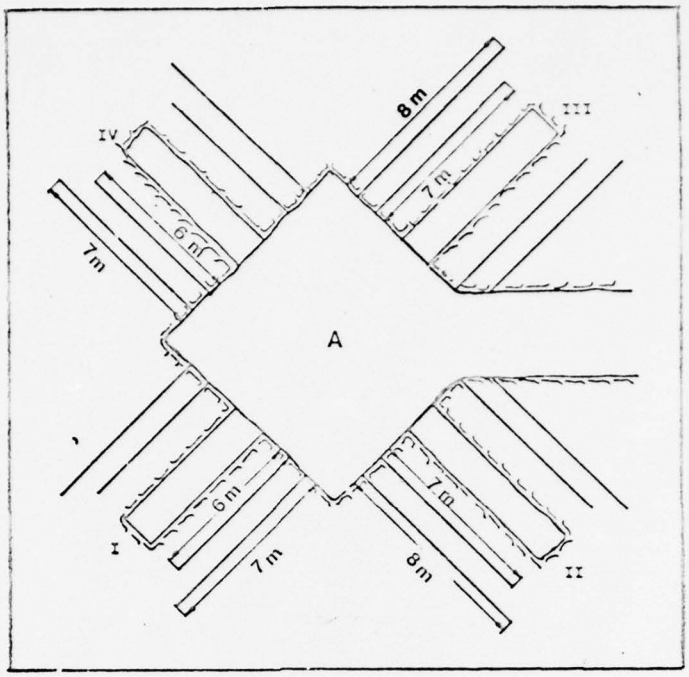

Fig.5 Geometry of the experiment. (Top view)

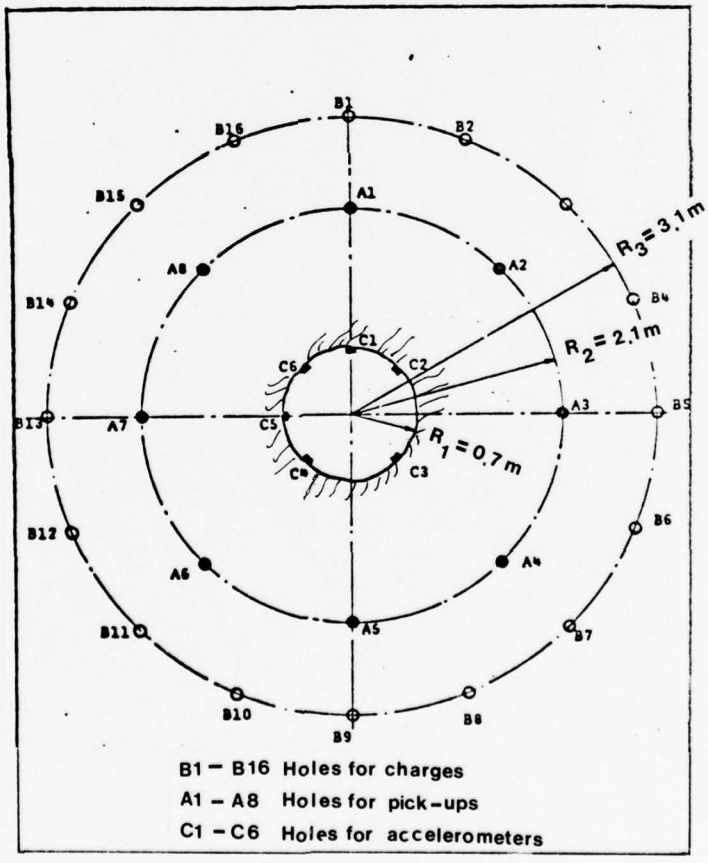

Fig.6 Geometry of the experiment. (View of the chamber wall.)

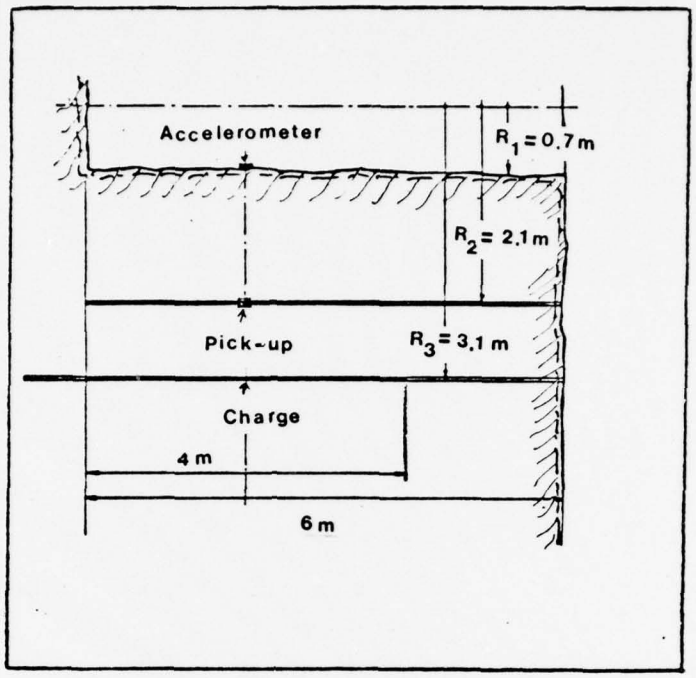

Fig.7 Geometry of the experiment. (Cut along the axis of the tunnel.)

may be influenced by the repeated detonations. Therefore the charges were raised from 30 to 120 [g/m] by tunnel II whereas it was decreased from 120 to 30 [g/m] by tunnel IV. The effect on the mass of the spall was striking. The two tunnels could be assumed to be rather equal and thus could be expected to behave similarly. The mass of the spall by 120 [g/m] was far less when this was the first detonation than when one had gradually increased the charge to the same value.

The influence of the method used to excavate the tunnels was also clearly brought out. The mass of the spalls in tunnels I and III which were drilled, was much less than in the other two which were blasted. If it were not for two discontinuity surfaces intersecting the drilled tunnels, where the only spalling took place, spalling would most probably not have occurred at all in these tunnels at the same level at which the others had to be considered "collapsed".

The pick-ups (based on strain gauges) and the accelerometers were used to monitor the shock wave. The measurements on the tunnel walls corresponded well with those made in the rock.

The results of these experiments beyond what has already been mentioned are perhaps best illustrated in the following diagrams. From the signals obtained by the accelerometers at the walls of the tunnels, the radial velocities at the walls could be obtained as functions of time. Fixing the attention on the peak values one found that the same charges measured in grams per meter (W) did not always create the same wall velocities in the tunnels. The peak values would also vary from one accelerometer to another. One may however take the mean peak value of the wall velocities and correlate with the charge magnitude as has been done in Fig.8 . One will then find that a rather nice correlation existed in the case of tunnels II, III and IV.

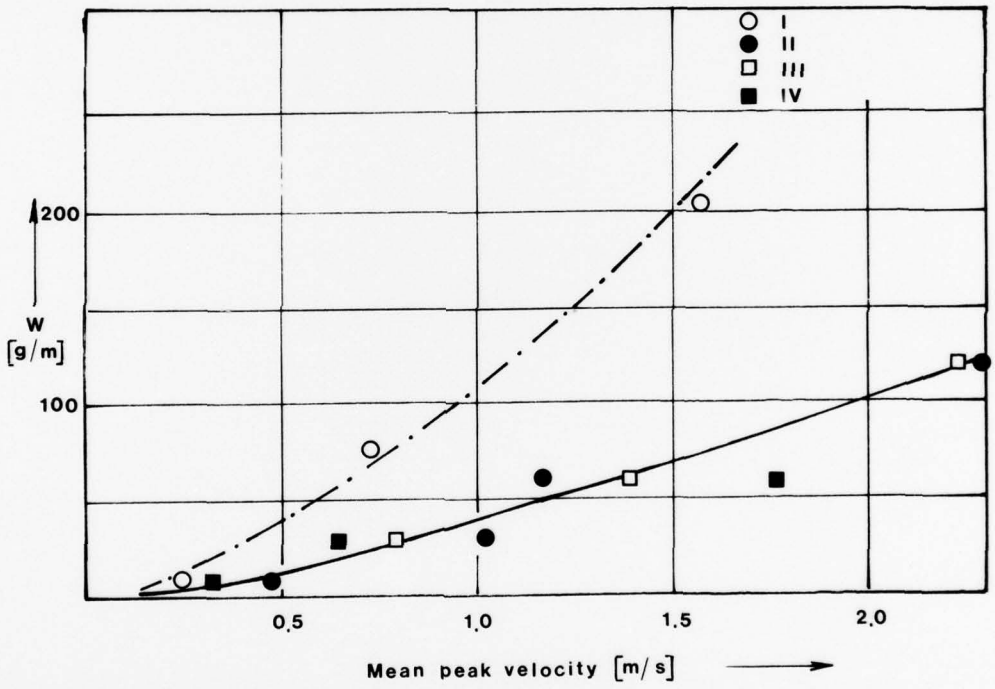

Fig.8 Correlation between charge magnitude W and the mean peak velocity created at the tunnel walls of the different tunnels.

It is however easily recognized that tunnel I deviates from the rest and thus the mean value of the peak radial velocities measured by means of the accelerometers at various locations for one shot should be correlated with the magnitude of the spalling caused by the shot. This is done in Fig.9 . The magnitude of the spalling is measured as the weight of the spalls (M) and Fig.9 reveals that now tunnel III

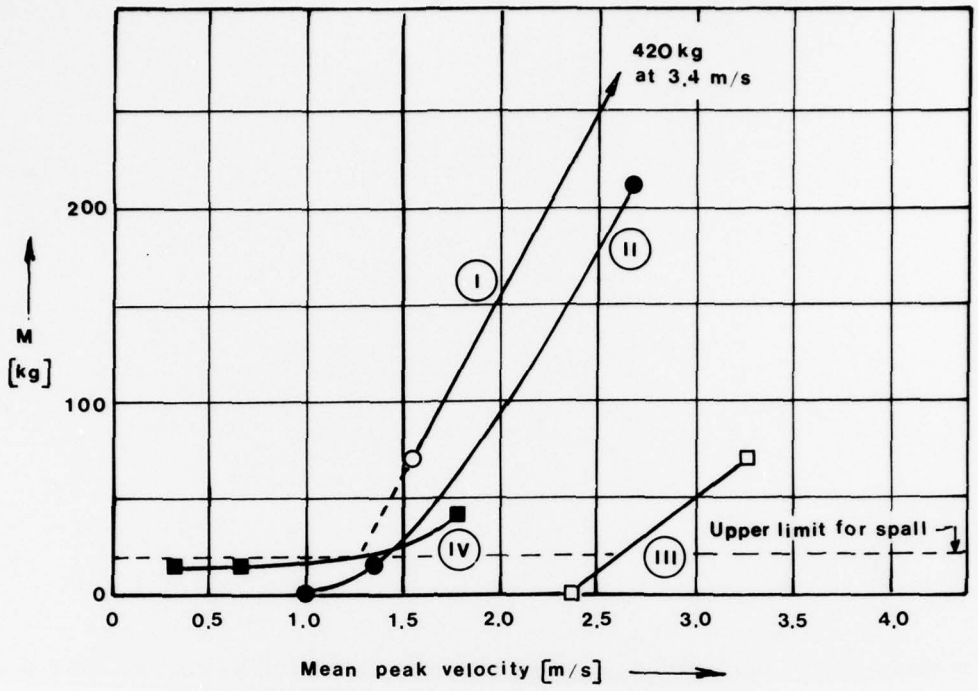

Fig.9 Mass of spall M shown as function of the mean peak velocity measured at the wall for each shot

seem to deviate from the others. It should however be kept in mind that the tunnels I and III were drilled, and that spalling in these tunnels took place only at the locations were these tunnels were intersected by the discontinuity surface in the rock. The result in Fig.9 for these tunnels are thus not representative for a tunnel drilled in the undisturbed rock.

The limiting value of *M* below which the spall is considered to be of tolerable magnitude has to be judged, and will sometimes depend on other considerations than the functioning of the tunnel as such. In Fig.9 this limit is chosen such that the limiting value is reached when the peak wall velocity is 1.4 [m/s]. This corresponds to a maximum amplitude of the oncoming shock wave of 103 [atm], which is less than 1/3 of the value obtained in the previous case.

One may now sum up the results of these investigations in the following points valid for raw tunnels:

1. It has been verified that the method used to excavate the tunnel will greatly influence the collapse criterion of the tunnel.
2. This means however in view of the long terms changes in the state of static stress around the tunnel, that also the age of the tunnel will influence the collapse criterion of the tunnel.

3. Using test tunnels on location and performing the described type of tests on them may for a given location give an indication of the collapse criterion in the sense used here. However, the uncertainties of such a procedure are so great, that one must contemplate very carefully if the expenditures are warranted.

2. The lined tunnel.

The experimental investigations of the collapse criterion of lined tunnels to be reported on here were all carried out in the same rock. Because one had to limit the number of possible types of linings to a managable number, only the types exhibited in Fig.10 were considered. These represent the normal types of linings used when more sophisticated arrangements are not needed.

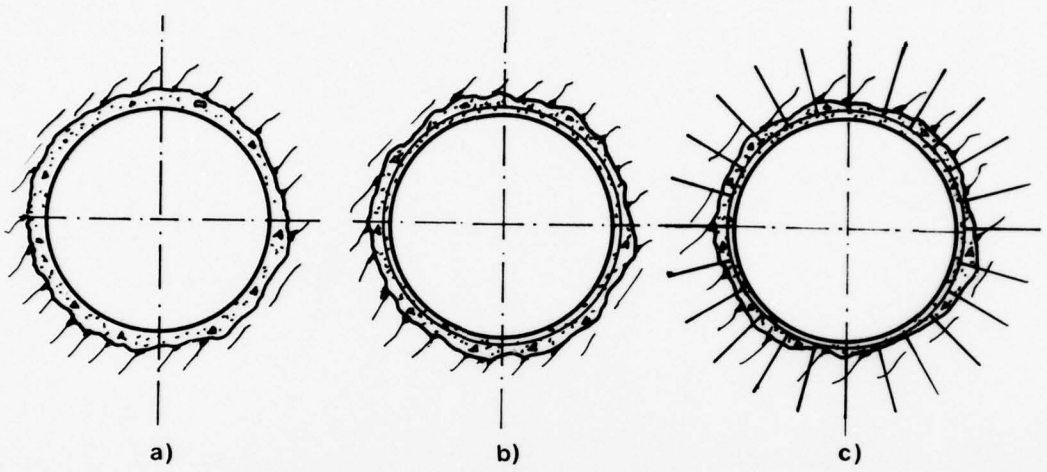

Fig.10 Lined tunnels to be tested. a) Concrete lining b) Reinforced concrete lining c) Reinforced concrete lining with anchors

Because the tunnels must be expected to be subjected to the shock waves from sherically symmetric sources, the geometry of the experimental set-up was chosen such that the test tunnels would be subjected to spherical shock waves. It was also decided, that because one would in most cases want to test tunnels in scales less than 1:1, the arrangement should preferably be such as to give information on the influence of the size of the tunnel radius. What could be called a model law for such experiments was envisaged.

In addition to the questions outlined above, main emphasis was to be placed upon an evaluation of the importance of anchors, i.e. how much would the carrying capacity of the tunnel be increased by the introduction of anchors as compared with the same lining without anchors. A similar consideration was also to be made to determine the importance of the reinforcement.

These considerations led to a geometry of the experiment which is sketched in Fig.11. In the floor of a large chamber were

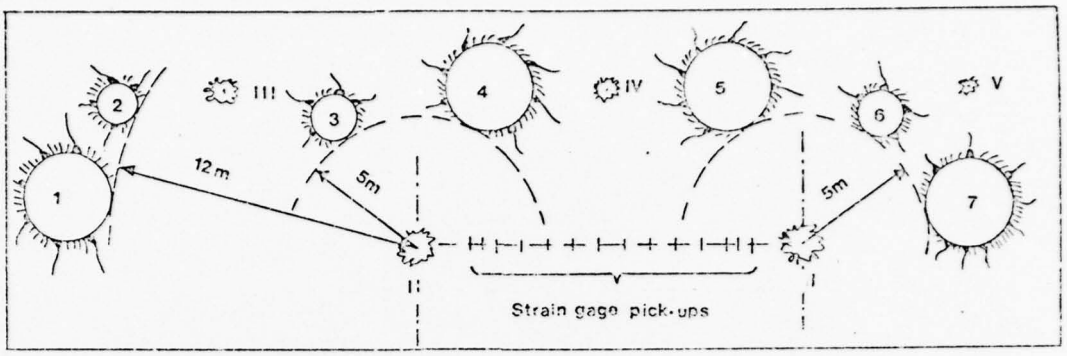

Fig.11 Sketch of the geometry of the experimental set-up.

excavated seven vertical tunnels numbered 1 through 7. Tunnels 1, 4, 5 and 7 had radiae of R = 1.7 [m], tunnels 2, 3 and 6 had radiae of R = 0.85 [m]. Tunnels 1 and 2 were unlined ("raw"), tunnels 3 and 4 were lined as b), tunnels 6 and 7 were lined as a) and tunnel 5 as c), a), b) and c) referring to the type of lining shown in Fig. 10.

These tunnels were to be subjected to shock waves created in I and II, two wells into which the charges were to be detonated. One could not, for practical reasons, make these wells so small that the charges to be used could be conceived of as completely confined. The charges were therefore detonated hanging free in the center of the wells which were filled with water. In this way it was also hoped to create identical shock waves in I and II using the water to transmit the input pulse to the rock. For testing the measuring devises small confined charges were detonated in III, IV and V, which were small holes drilled in the rock. The distance from the main charge in I or II to the tunnels was 5 [m] as shown in Fig.11 . However, the unlined tunnels 1 and 2 were placed at a distance of 12 [m] from II, because their capacity to withstand the effect of the shock wave was estimated to be far less than the lined tunnels'.

The tunnels were 10 [m] deep as shown in Fig.12 . They were lined to a height of 6 [m] above the floor. The charges were always placed at a depth of 7 [m] below the top surface, at which depth the measuring sensors were placed. These sensors consisted of accelerometers attached to the tunnel walls as shown in Fig.13. In addition a row of strain gauge based pick-ups were placed between the two wells for the charges. The signals from these were used to get information on

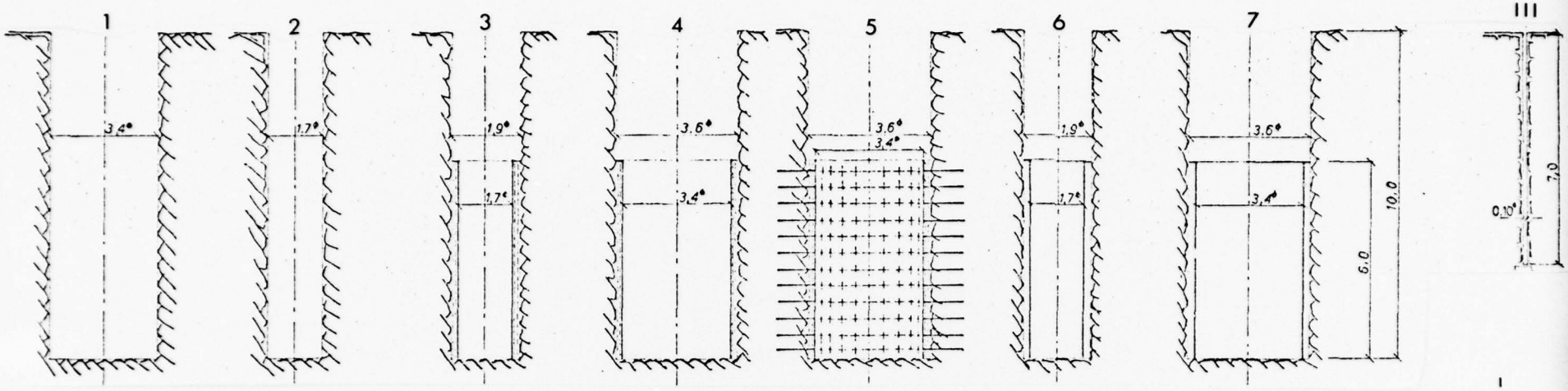

Fig. 12 Side view of the tunnels (cut through the centerline), charge hole III

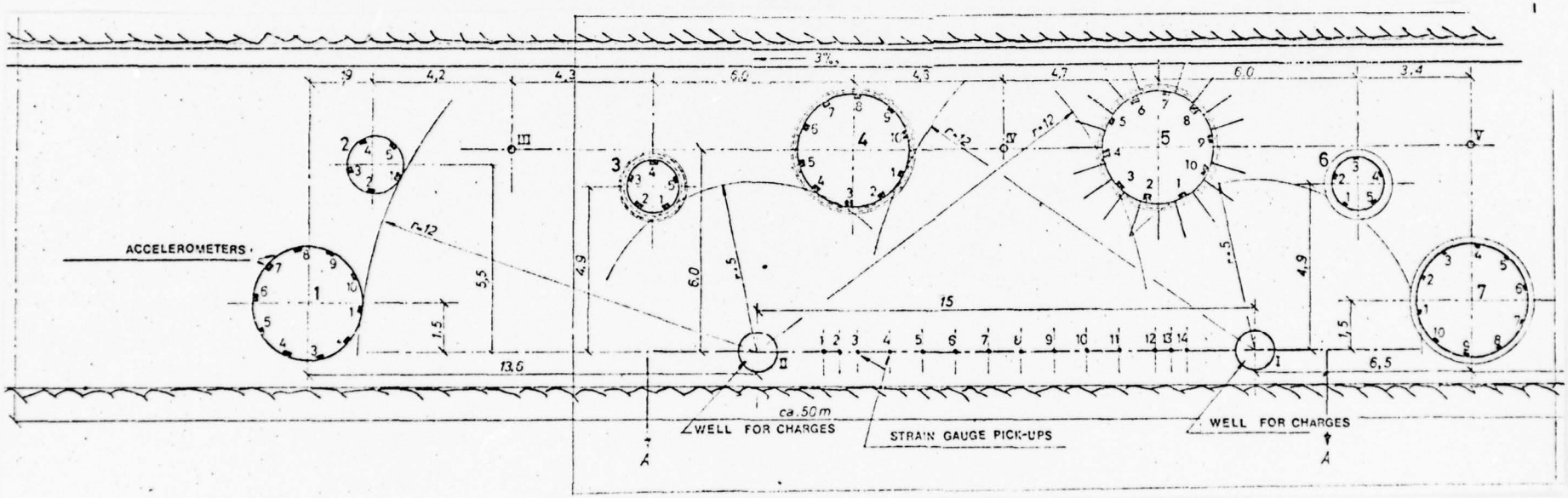

Fig. 13 Top view of the tunnels showing the positions of the accelerometers.

the shock wave created in each case by the explosion. From the accelerometer signals information could be obtained on the motion of the walls and the maximum amplitude of the shock wave when reaching the tunnel could be determined.

The intention was to use charges large enough to bring the tunnel wall to failure. The maximum amplitude of the stress wave as it reached the tunnel could then be used as a collapse criterion. One would however have to try to get failure at the first attempt because the previous experiments had shown a marked influence of repeated explosions. One started out with 1 and 2 kg charges in III, IV and V for calibration purposes. It was however decided also to detonate smaller charges in I and II for the same purpose, but because of the way in which the shock wave was created the charges were here 10 kg.

The first real test was the detonation of 50 kg TNT in II. This was done to fix at least one lower level which was not dangerous to the tunnels. No visible damage was done to any tunnel on this occasion. Then 200 kg TNT was detonated in I and thereafter in II. In these cases heavy damage was inflicted on all tunnels except the unlined tunnels 1 and 2, which remained intact due to the longer distance from the source.

Some conclusions were drawn from inspection of the damages:

1. Comparison between tunnels of different sizes but with the same type of lining (tunnels 3 and 4 and to some extent also tunnels 6 and 7) showed that the yield mechanisms were basicly the same in both cases. The damages seemed however to be greater in the lager tunnels, an observation which will be given some thoughts later.
2. Comparison between tunnels of the same size but with different types of lining (tunnels 4, 5 and 7) showed that the damages inflicted on tunnel 7 (concrete lining without reinforcement) were much larger than for the other two. Tunnel 7 collapsed completely as is seen from the photo in Fig.14 . It was concluded that in most cases would this kind of lining contribute very little to increasing the tunnel's capasity to withstand the influence of the shock wave.
3. The yield mechanism by lined tunnels under these conditions may be contemplated by observing the fracture of the walls of tunnel 4 shown in Fig.15.
4. The fracture of tunnel 4 is similar to that of tunnel 5. The difference in the lining of the two tunnels consists of the anchors and one may conclude that although the anchors may have contributed to change the stress pattern slightly, the collapse criterion is for all practical purposes the same. The influence of the anchors is therefore marginal.

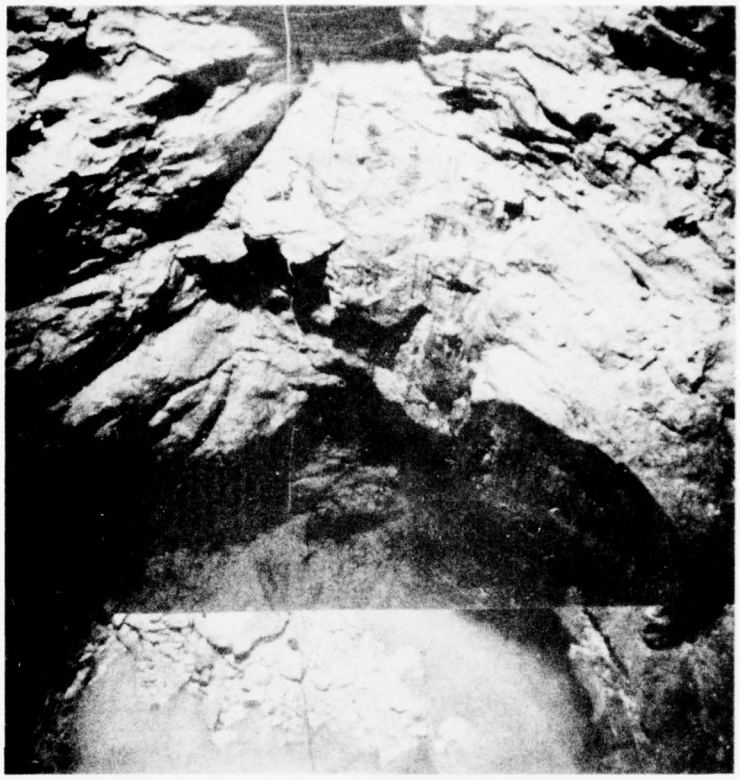

Fig. 14 View of tunnel 7 after the 200 kg shot. The tunnel has collapsed completely and only a small portion of the original wall can still be identified.

Fig. 15 View of tunnel 4 after the 200 kg shot. The yield occurred at two distict generatices. The yield mechanism is shown skematically in Fig. 16

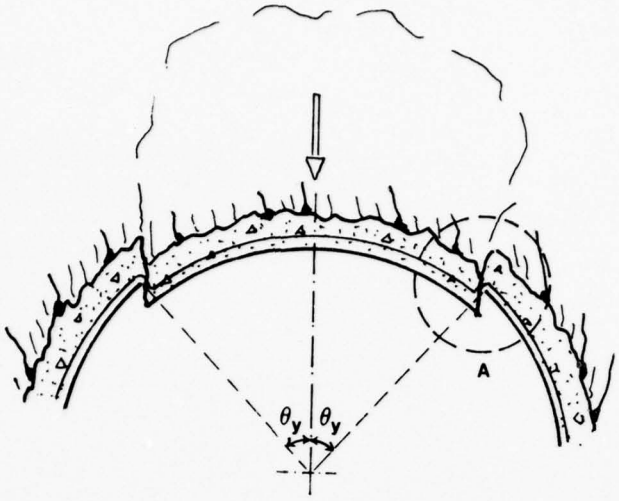

Fig. 16 Sketch showing the yield mechanism. Circle A corresponds to circle A in Fig. 17.

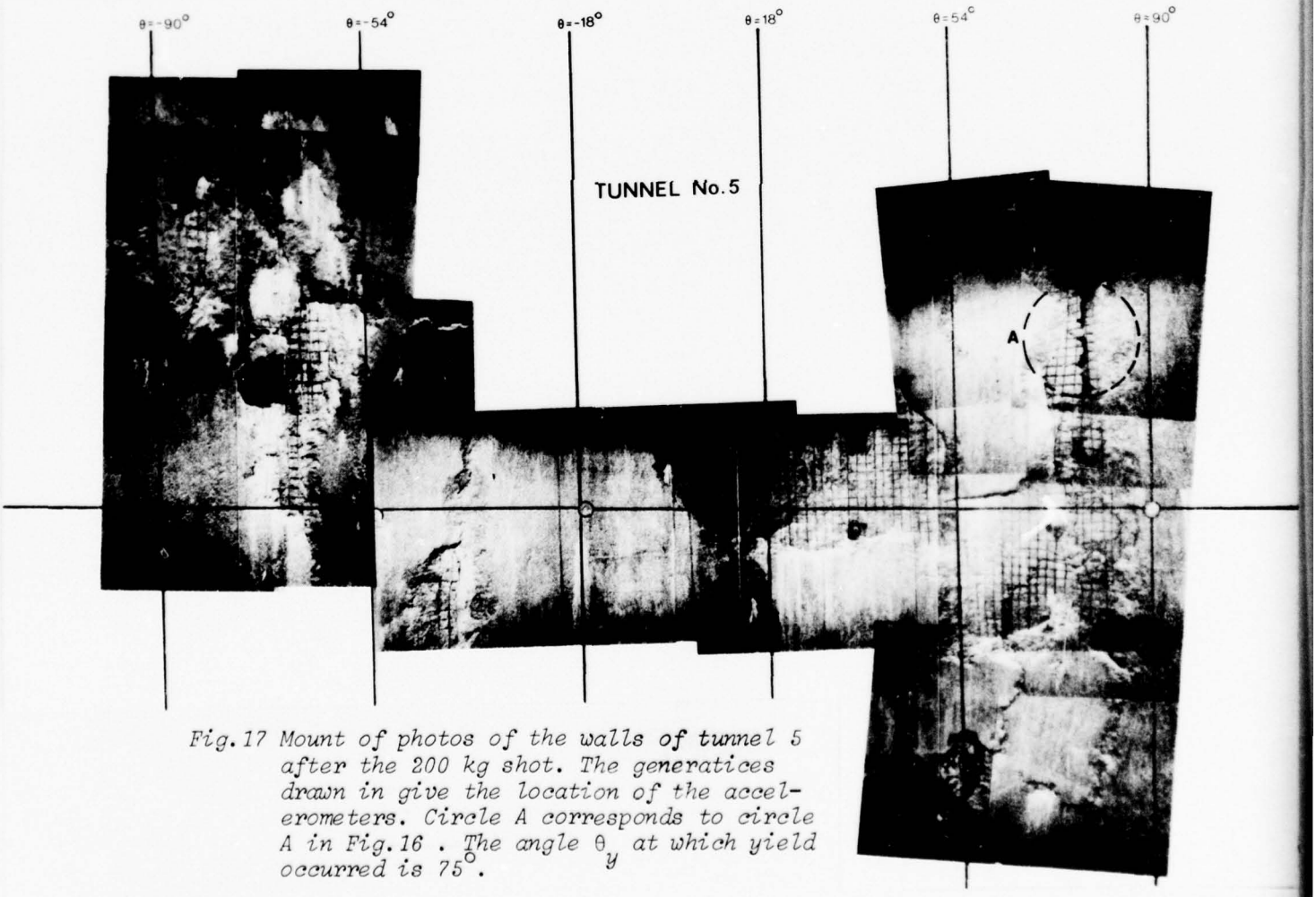

Fig. 17 Mount of photos of the walls of tunnel 5 after the 200 kg shot. The generatices drawn in give the location of the accelerometers. Circle A corresponds to circle A in Fig. 16 . The angle θ_y at which yield occurred is 75°.

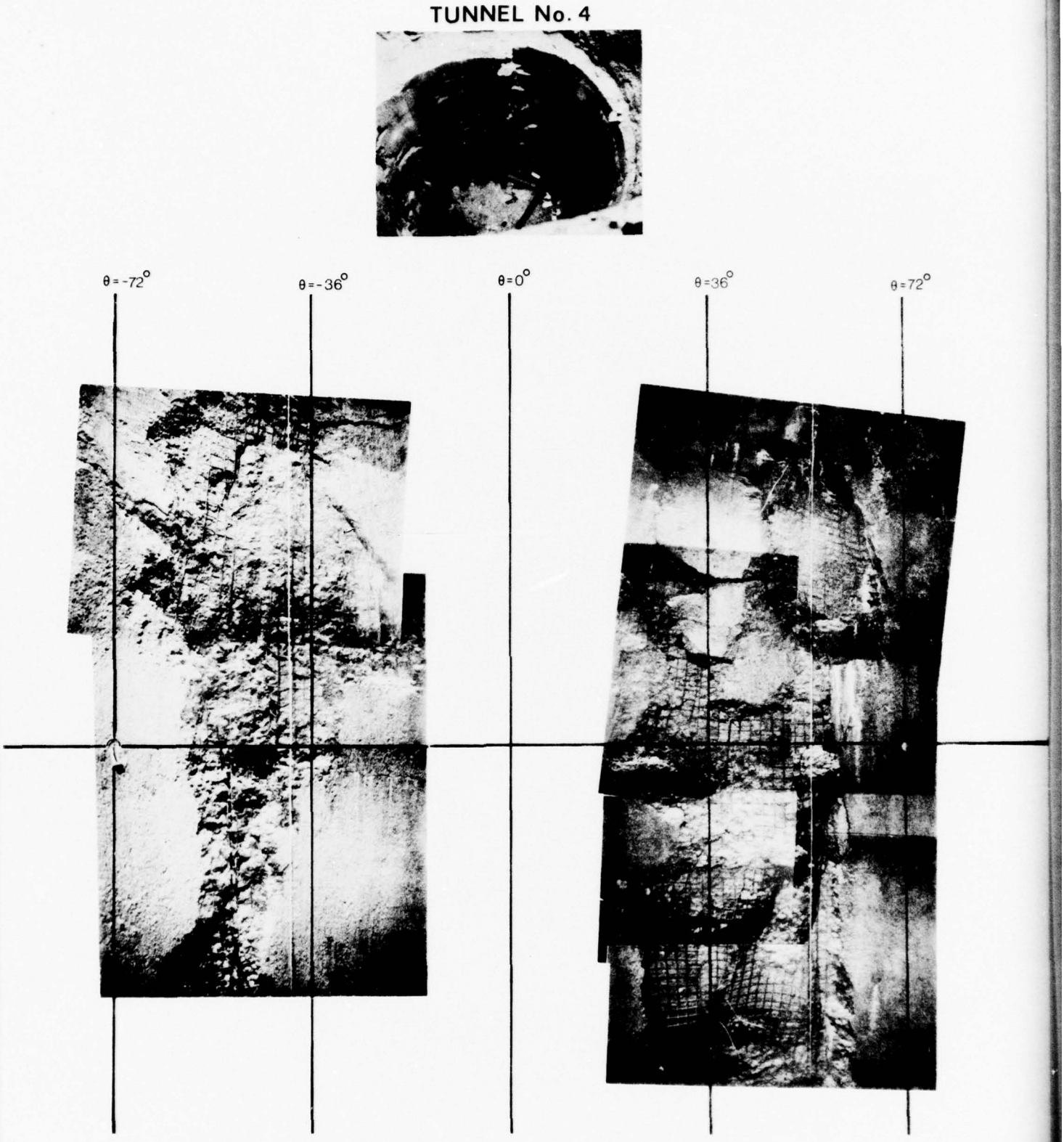

Fig. 18 Mount of photos of the wall of tunnel 4 after the 200 kg shot. The yield occurred as in tunnel 5 but the yield zone is here located at $\theta_y = 54^\circ$. The generatices shown indicate the location of the accelerometers.

The yield mechanism suggested by the fracture zones of tunnels 4 and 5 is given as a shear fracture in Fig.16 . This occurs along generatrices as clearly indicated by the photo mounts in Figs. 17 and 18. One observes of course spalling also elsewhere on the walls whereby the reinforcement is uncovered, but the real fracture of the lining occurs at an angle θ_y. This angle is different in the two tunnels (75° in 4 and 54° in 5) and this may be attributed to the influence of the anchors. In a later section this will be dicussed in context with an attempt to explain the fracture in detail.

The smaller tunnels 3 and 6 were also brought to collapse. The damage inflicted upon them did not seem to be as great as for the same type of tunnel with a larger radius. Fig.19 shows tunnel 6 after

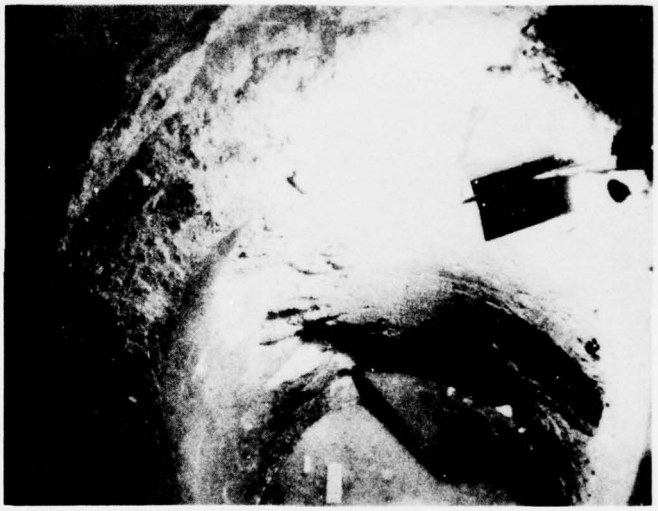

Fig.19 View of tunnel 6 after the 200 kg shot. The fracture takes place along generatices as in the case of tunnel 4

the 200 kg shot. The tunnel should be compared with tunnel 7, a tunnel with the same lining but with a larger radius. Tunnel 7 collapsed completely, tunnel 6 showed collapse with damage comparable to tunnel 4 and with fracture occurring along generatrices. It should be noted, that the thickness of the lining was the same in tunnels 6 and 7, and that the thicknes/radius ratios were different in the two cases. This will later be used to explain the difference in the damage.

Fig.20 shows tunnel 3 after the 200 kg shot. This tunnel had the same lining as tunnel 4, it collapsed in the same way as this

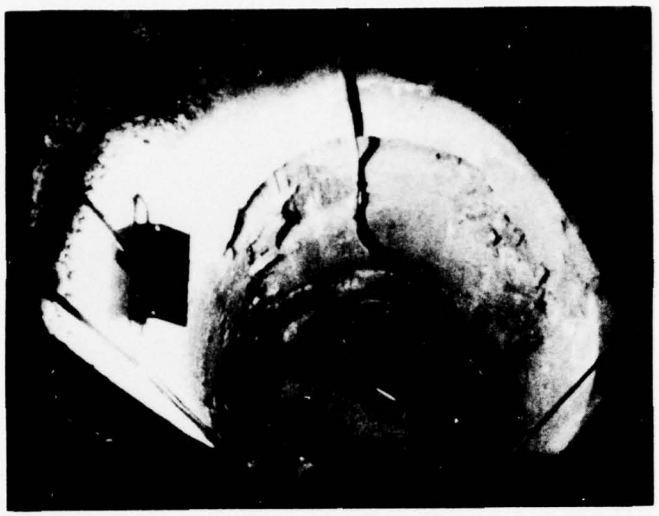

Fig.20 View of tunnel 3 after the 200 kg shot. The fracture takes place along generatrices as in the case of tunnel 4

tunnel and again the damage was observed to be smaller for the tunnel with the smaller radius. All comments to tunnel 6 apply also to this case.

This concludes the remarks on the damages as such and represent also the answer to some of the questions originally posed. However, the instrumentation gave additional information of quantitative nature which could be used to supplement the information obtained so far. Such information would concern the wall velocities created by the shock wave etc. For that purpose the undisturbed tunnels 1 and 2 were equipped with a lining of the type b) in Fig.10 and subjected to the influence of shock waves created in a well as described here. For further supplementation the lining was doubled in thickness to see if the effect of the thickness of the lining could be detected in the results. Again the tunnels were subjected to the influence of shock waves, whereby in both cases the maximum amplitude of the shock waves was kept low enough to avoid damage to the linings. The results of these experiments are described in the following section.

3. The wall motion.

The experiments described so far had the aim to provide answers to rather limited questions, but as mentioned one found that answers of greater generality might perhaps be found. Hence the extention of the experiments was approved.

One finds that cases may occur in which the contents hidden in the shelter and their sensitivity determine the extent to which the tunnel may be subjected to the influence of shock waves. Thus cases may occur where the "collapse criterion" is an upper bound on the maximum permissible amplitude of the shock wave at the tunnel which is far below the value for which the tunnel as such is endangered. The way in which the contents will experience the shock wave will depend on the arrangement within the tunnel, but in all cases the motion of the tunnel walls during the period when the tunnel is engulfed by the shock wave will be of significant importance.

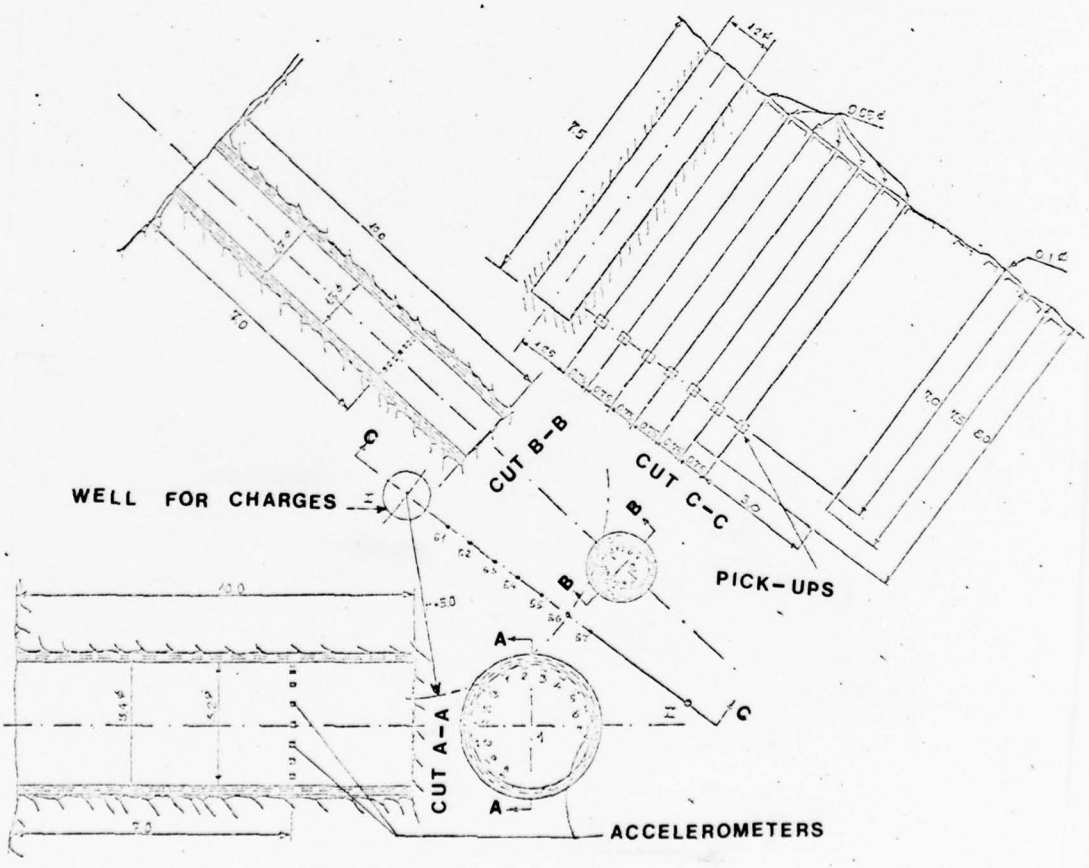

Fig.21 Geometry of the supplementary experiments showing the two test tunnels 1 and 2, the well for the charges and the row of strain gauge based pick-ups for monitoring the stress wave.

The geometry of the supplementary experiments is shown in Fig.21 . It is noticed that the tunnels are now equipped with accelerometers mainly on that side which faces the oncoming shock wave. The reason for that is that in the first experiments very little movement of the "back walls" was recorded even in the cases where the "front walls" were heavily damaged. It should be noticed that this indicates a special type of collapse , and that thus the results are limited to this situation.

Before going into detail on the results the following considerations are useful. The interaction between a shock wave and a tunnel will to some extent be characterized by the ratio D/L between the diameter D of the tunnel and the length L of the oncoming shock wave. When $D >> L$ the interaction will be similar to the reflection from a plane wall, and the maximum amplitude of the stress wave may have been considerably attenuated when travelling a distance equal to the diameter of the tunnel. Usually this situation is not of any great practical importance. When $D << L$ the variation in the stress across the tunnel is not significant compared with the stress level in the wave. One has a quasi-static case with a stress distribution around the tunnel which may be judged from static considerations. This may be the case when the stress wave originates from a nuclear source. When $D \simeq L$ the situation occurs which the experiments are supposed to cover, and which is rather difficult to handle theoretically. In the tests carried out in the experiments the ratio varied within the range $1.36 < L/D < 5.67$.

The scope of the investigation was to establish relations which would permit the prediction of the motion of the tunnel walls when the oncoming shock wave was specified. Such a specification can be given by 3 quantities if the oncoming wave is considered to be mainly a triangular wave as shown in Fig.22 . The maximum amplitude A is measured in [m/s] whereas the wave length L and the rising length ΔL are measured

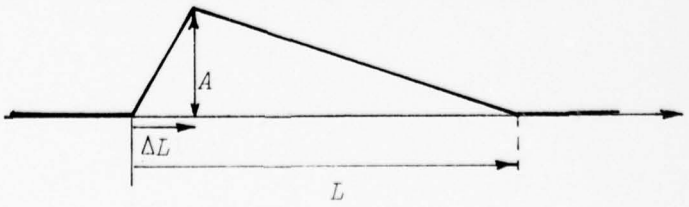

Fig.22 Simplified form of the oncoming shock wave

in [s] and converted to lengths by means of the signal velocity c_s of the rock. This really means that the shock wave is characterized by its velocity field.

One should bear in mind that measurements of wave lengths are very uncertain and that great care must be exercised when deciding whether or not irrelevant influences are present in the signals. As an example Fig.23 shows the signals for shots 4 - 8 with the triangular wave drawn in. The "tail" of the original signal is influenced by reflections and has therefore been neglected in deciding the triangular replacement wave.

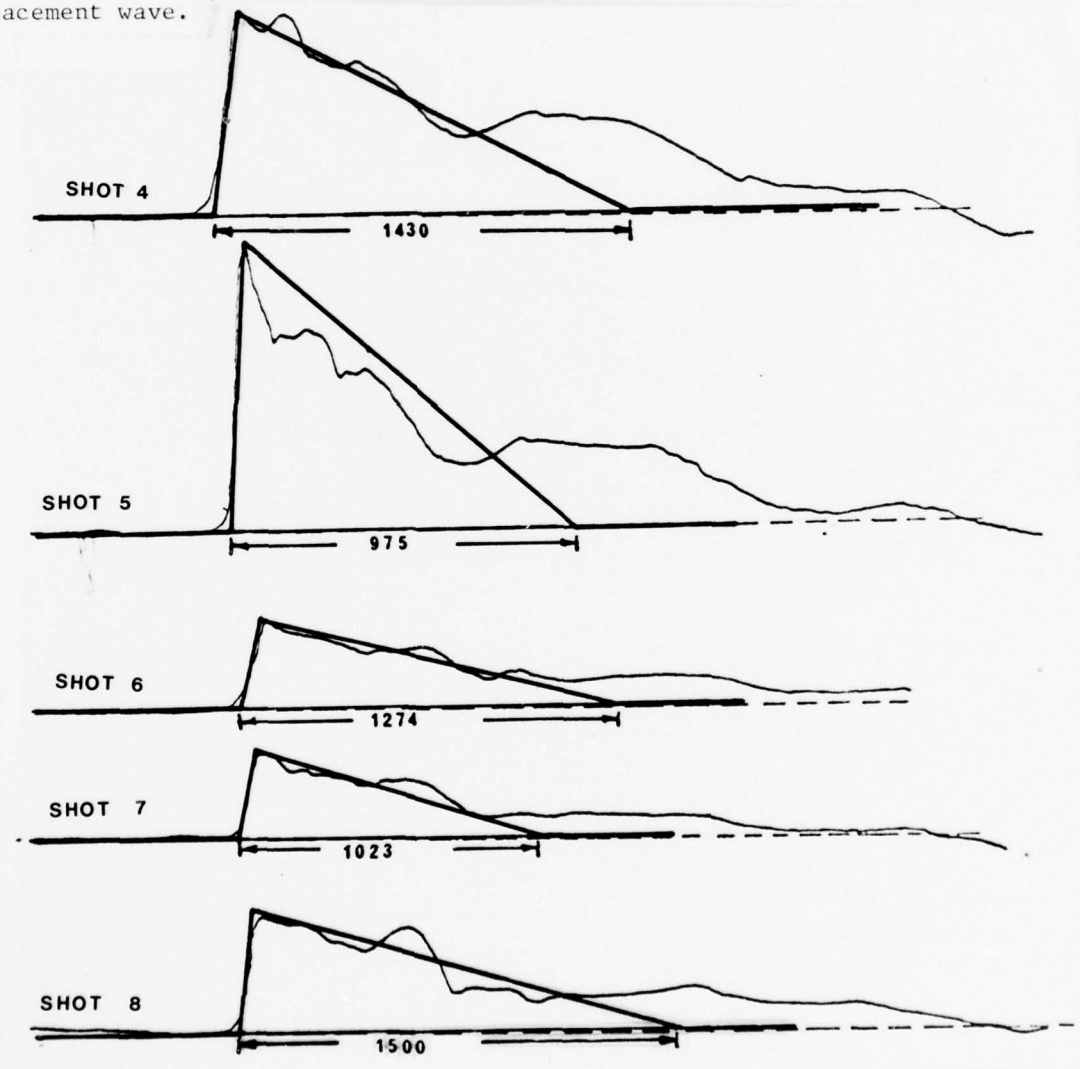

Fig. 23. Wave forms by shots 4 - 8 with their triangular replacement waves.

With the three input data A, L and ΔL in addition to the signal velocity c_s of the rock the motion of the tunnel walls can be predicted in the following sense:

1. Just as attention is fixed only at the first positive phase of the oncoming shock wave, only the first positive phase of the radial wall velocity V_r is considered.
2. The first positive phase of V_r is conceived of as having a triangular form.
3. The wall motion will then be given by four quantities:

   $V_{r,max}$ given as a function of the location θ, θ being the angle at the center of the tunnel between the direction to the source and the direction to the location.

   t_a given as the time at which motion at the location θ starts.

   t_r given as the rising time, i.e. the time needed for V_r to reach its maximum value at location θ.

   Δt given as the duration of the positive phase of the radial wall velocity at location θ .

The aim is to relate these four quantities to the three parameters of the shock wave.

The arrival time t_a :

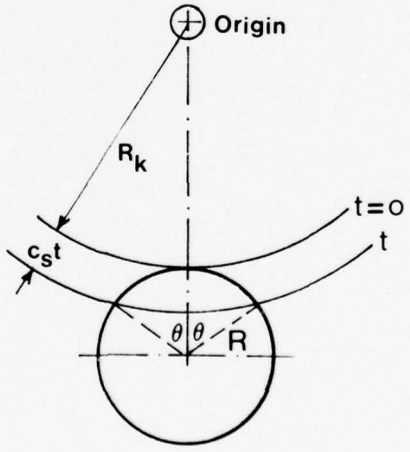

Fig.24 Geometry of a spherical shock wave engulfing a cylindrical cavity.

The arrival time t_a is counted from the time when the shock wave first meets the cavity until it has reached the position θ as shown in Fig.24. From purely geometrical considerations one obtains:

$$\frac{c_s t_a}{R} = \frac{R_k}{R}\left\{\sqrt{1 + 2\left[\frac{R_k}{R} + \left(\frac{R_k}{R}\right)^2\right](1 - \cos\theta)} - 1\right\} \quad (3.1)$$

This may be replaced by the much simpler expression when $R_k >> R$:

$$\frac{c_s t_a}{R} = (1 - \cos\theta) \quad (3.2)$$

The maximum amplitude $V_{r,max}$

The maximum amplitude $V_{r,max}$ of the radial component of the wall velocity may according to the findings of the investigations be expressed as follows:

$$V_{r,max} = V_o \exp\left(-\left(\alpha\frac{\theta}{180}\right)^2\right) \quad (3.3)$$

where α is a constant expressing the influence of the size of the tunnel and where θ is to be introduced in degrees ($^\circ$). The size of the tunnel is related to the decay of the stress wave as it travels a distance comparable to the radius of the tunnel. Let S_o be the non-dimensional peak stress in the shock wave as its front impinges on the tunnel. Let S_{90} be the corresponding value when the wave has travelled so far that its front has reached the position $\theta = 0$. Then α is given by:

$$\alpha = 1.784\ S_o/S_{90} + 0.256 \quad (3.4)$$

It is clear that in this way not only the size of the shock wave as compared with the tunnel, but also the "properties" of the rock as a wave transmitting medium has been attempted accounted for.

The duration time Δt :

The duration time Δt of the first positive phase of the radial wall velocity may be expressed as follows:

$$\Delta t = \Delta t_o \exp\left(-\left(\beta\frac{\theta}{180}\right)^2\right) \quad (3.5)$$

where β according to the results seem to be independant of the tunnel size and consequently equal to a constant:

$$\beta = 2.25 \tag{3.6}$$

The quantity Δt_o is the duration time recorded at the location $\theta = 0$, and it may be related to the oncoming shock wave as follows:

$$\Delta t_o = \frac{L}{c_s} \tanh(5R/L) \tag{3.7}$$

where R is equal to the tunnel radius as before and L is the wave length of the shock wave in the sense used previously.

The rising time t_r :

The time needed for the velocity at a given location to increase from zero to its first peak is called the rising time t_r and may be given as a fraction of the duration time:

$$t_r/\Delta t = 0.059 + 1.510(\theta/180)^2 \tag{3.8}$$

The numerical constants in this expression are rather uncertain. They have been determined from information from the first experiments in the geometry shown in Fig.11, and Fig.25 gives an impression of the accuracy.

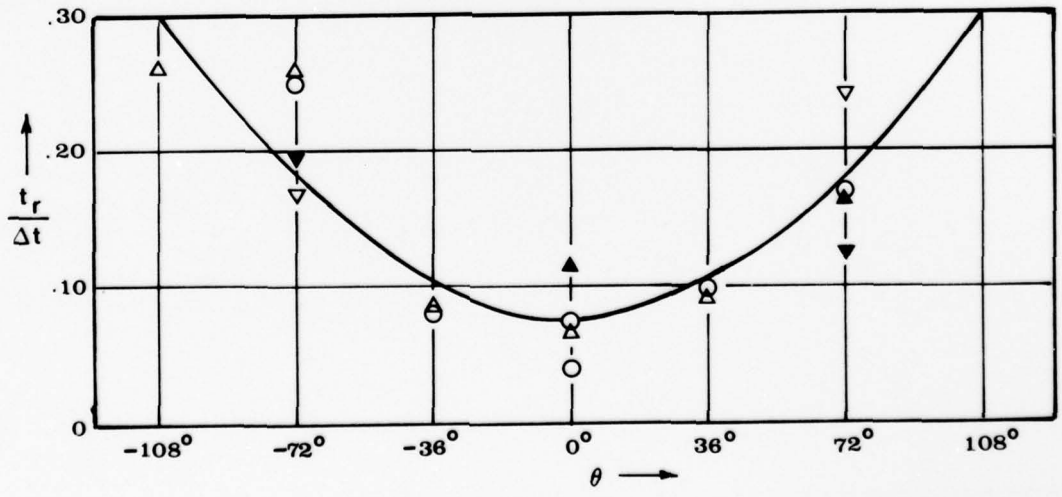

Fig.25 The ratio $t_r/\Delta t$ plotted as function of θ. The curve represents equation (3.8)

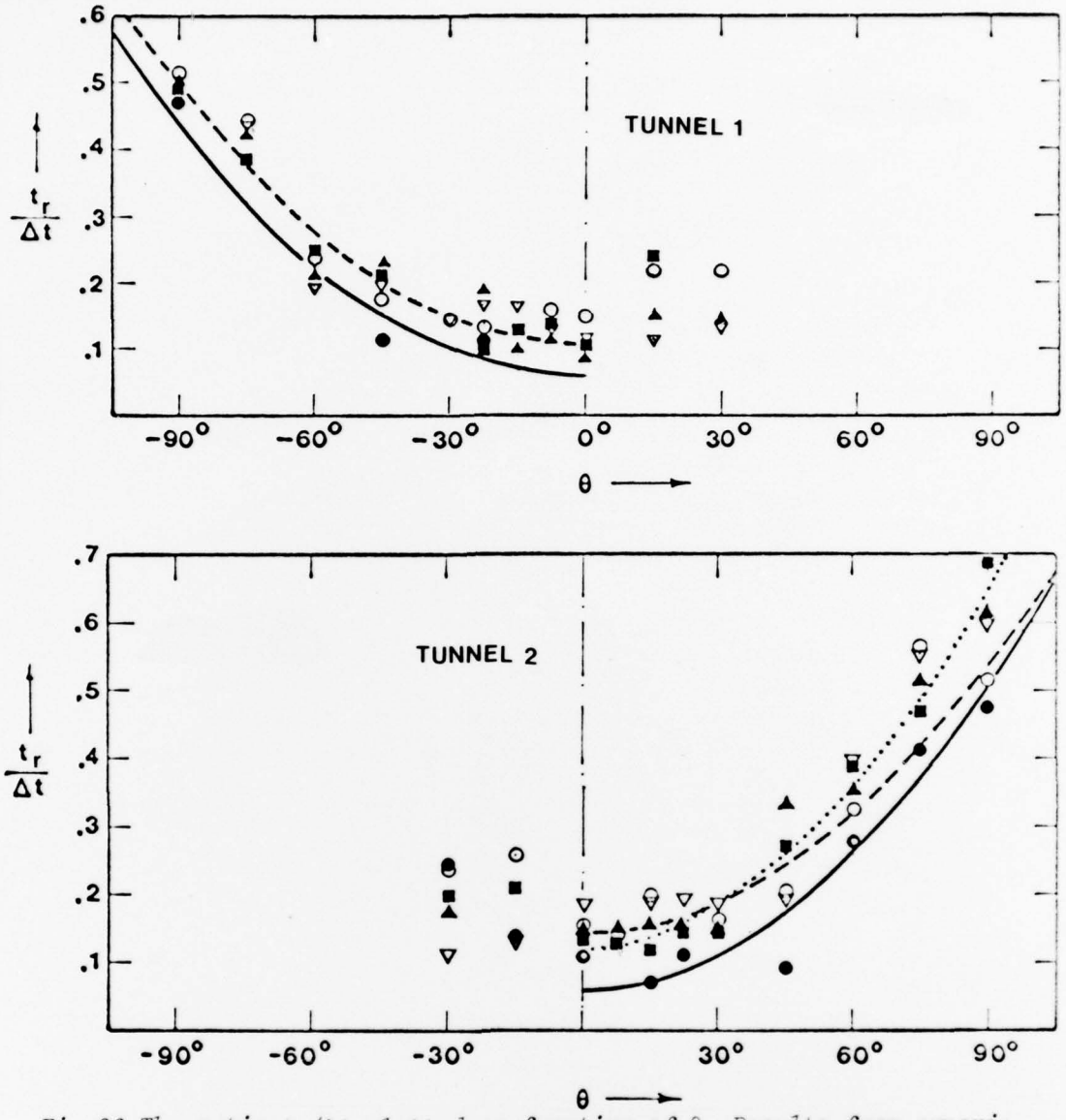

Fig.26 The ratio $t_r/\Delta t$ plotted as function of θ. Results from experiments in the geometry of Fig.21

------ $t_r/\Delta t = 0.1477 + 1.560(\theta/180)^2$ *(Tunnel 2)*

------ $t_r/\Delta t = 0.1079 + 1.552(\theta/180)^2$ *(Tunnel 1)*

····· $t_r/\Delta t = 0.1318 + 2.078(\theta/180)^2$ *(Tunnel 2)*

——— $t_r/\Delta t = 0.059 + 1.510(\theta/180)^2$ *(Tunnels 1 and 2)*

The later experiments in the geometry of Fig.21 gave results exhibited in Fig.26. The uncertainty of the constants is clearly demonstrated. It should be noticed that this uncertainty is immaterial for the determination of the maximum radial displacement of the wall, it is however crucial if one wants to determine the maximum radial acceleration of the wall.

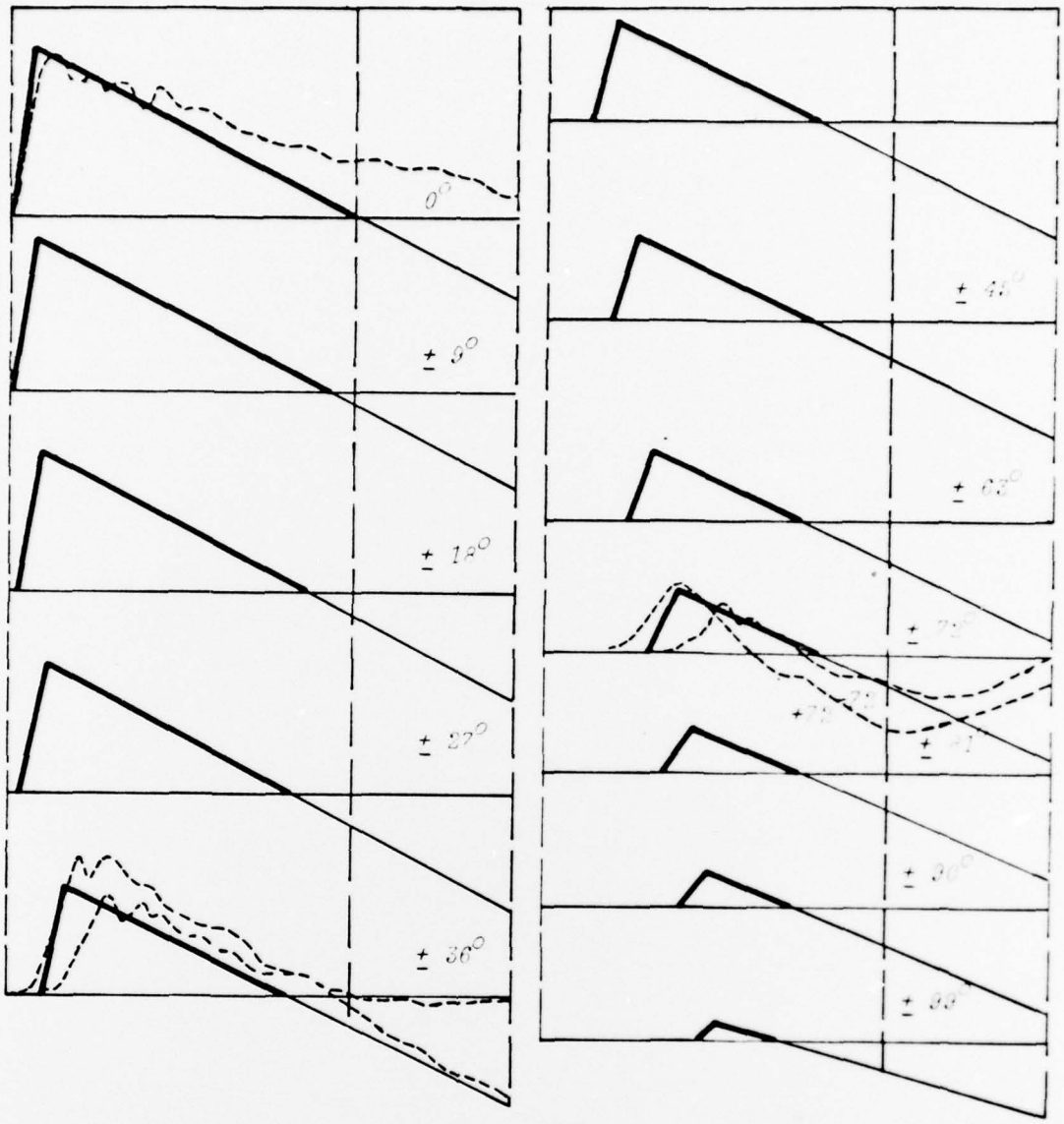

Fig.27 Comparison between measured wall velocities at tunnel 7 (---- dotted line) and the predicted velocities based on the equations (3.1) to (3.8) (——— full drawn line)

The way in which the empirical formulae (3.1) to (3.8) may be used is exhibited in Figs.27 and 28. In these diagrams the recorded wall velocities are shown as functions of time. These are compared with the signals which can be predicted based on the given formulae provided the oncoming shock wave is specified. Fig. 27 shows the comparison for the 50 kg shot against tunnel 7 where the shock wave specification has been gathered from the recordings made of the wave propagation. It should be noted that this is a tunnel with a large radius, and with a lining that did not stand up to the 200 kg shot. Fig.28 shows the

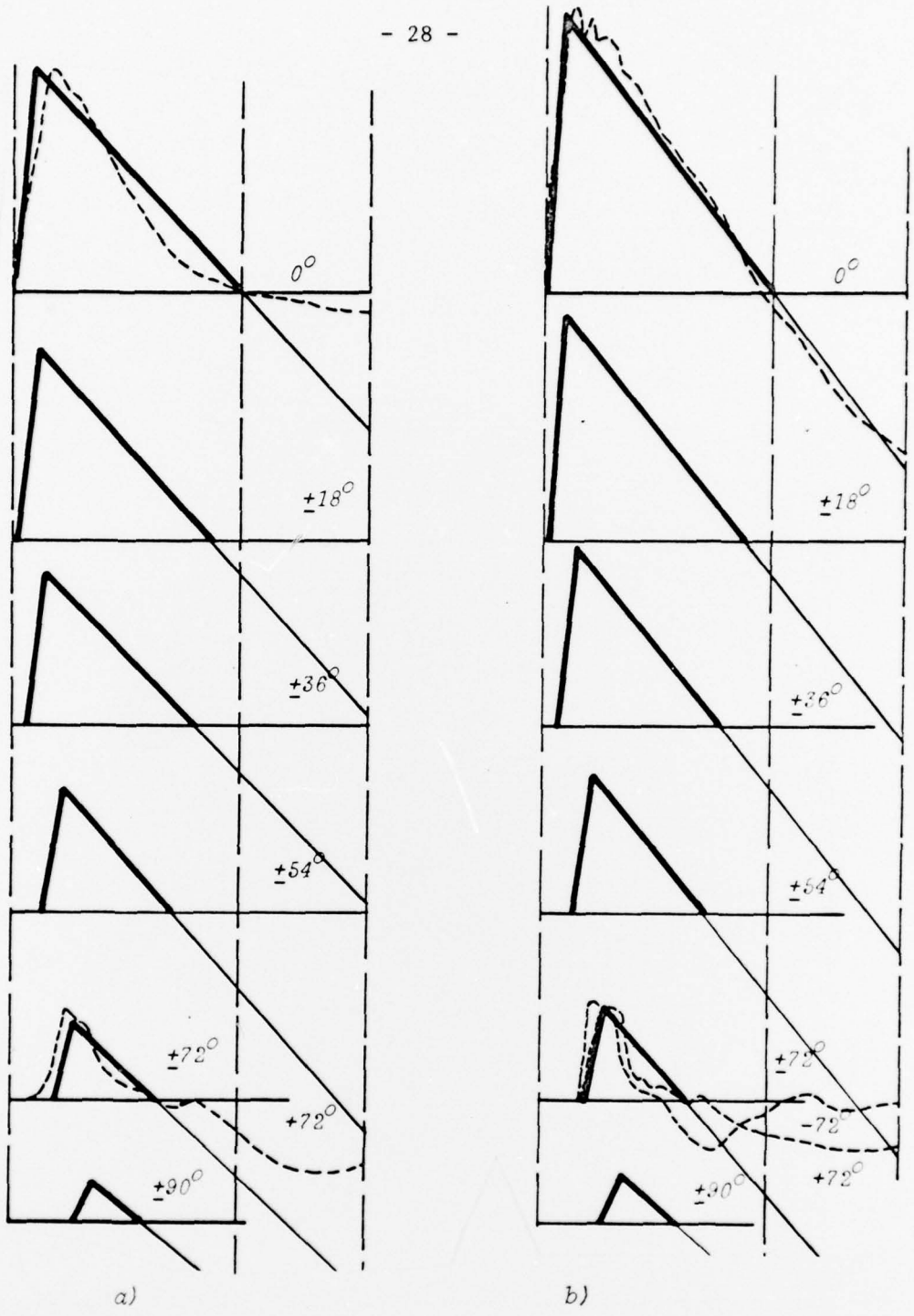

Fig. 28 Comparison between measured wall velocities at tunnel 3 (----- dotted line) and the predicted velocities based on equations (3.1) to (3.8) (——— full drawn line)

a) 10 kg charge

b) 50 kg charge

same type of comparison for tunnel 3 (Fig.11) which is a tunnel with only half the radius of tunnel 7 and with a different lining. It is seen that in both cases the predictions occur with a satisfactory degree of accuracy bearing in mind the great uncertainties of such measurements. It seems that the type of lining, at least within the variations considered here, does not influence the wall motion as long as the stresses are kept on a level below collapse.

4. A semi-static approach.

The investigations described here are only aimed at gaining an understanding of the collapse of a tunnel when this takes place as a puncture of the lining during the passage of the first phase of the shock wave. Only this case has been studied experimentally, and the empirical relations obtained are limited to such cases. However, it may be of interest to attempt a more detailed study of how collapse is brought about under such circumstances.

If one compares the carrying capacity of a "raw" (unlined) tunnel with that of a lined one, it seems natural to attribute the increased capacity of the latter to the fact that the lining is carrying the burden exclusively. The lining will act as a shell or an arch which during the passage of the shock wave carries a rapidly changing load. One may attempt computing the stresses in the lining by a static approach, assuming that, at each position of the shock wave relative to the tunnel, the lining acts as an arch carrying a static load which however would have to vary from one position to another. The problem will then be to determine the load to be applied.

In the following the situation will be examined when the front of the shock wave passes the front portion of the tunnel. The tunnel is supposed to have a circular cross section, the front of the shock wave has a given slope and its position during the passage is given by the angle θ_o as shown in Fig.29 . Two positions of the shock wave are shown in Fig. 29 , and the load function p giving the distribution of the load on the arch over its horizontal projection is supposed to be proportional to the amplitude of the shock wave in an undisturbed field. This

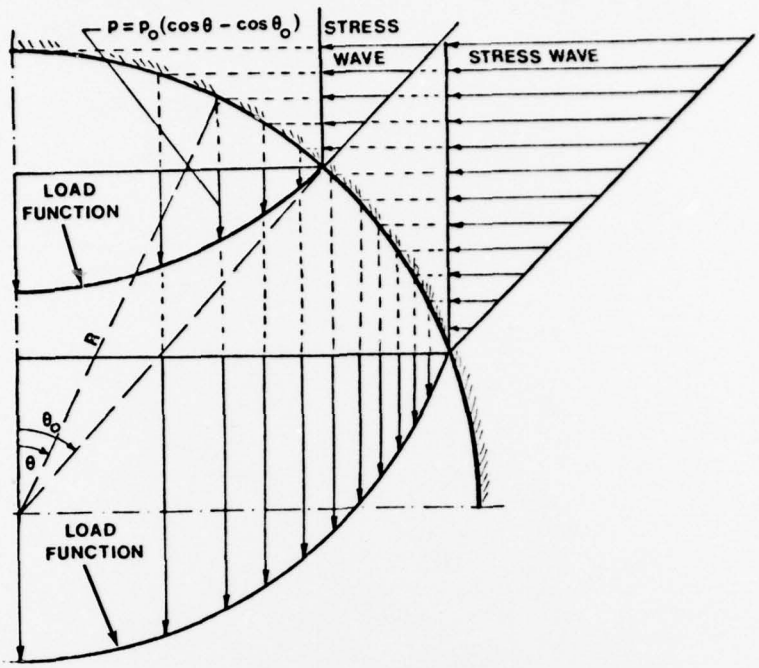

Fig.29 . The front of the shock wave at two positions $\theta = \theta_o$ with the corresponding load function p.

then leads to the following expression for the load function

$$p = p_o(\cos\theta - \cos\theta_o) \tag{4.1}$$

It should be stressed that this is to be regarded as a guess, and that a similar distribution

$$p = p_o \frac{1 - \cos\theta_o}{\sin\theta_o} (\sin\theta_o - \sin\theta) \tag{4.2}$$

would give a straight line distribution with the same value at $\theta = \theta_o$. This would be just as acceptable a guess for the load function, and consequently also this possible distribution will be considered.

It is further assumed that the lining acts as an arch which is built in at its ends where $\theta = \pm\theta_o$. The situation will then be as sketched in Fig.30 where the loading situation on the arch is given. H_o and V_o are the horizontal and the vertical components respectively of the force transmitted through the arch at its built-in end and M_o is the bending moment at the same location. At an arbitrary location θ the forces transmitted through a cross section

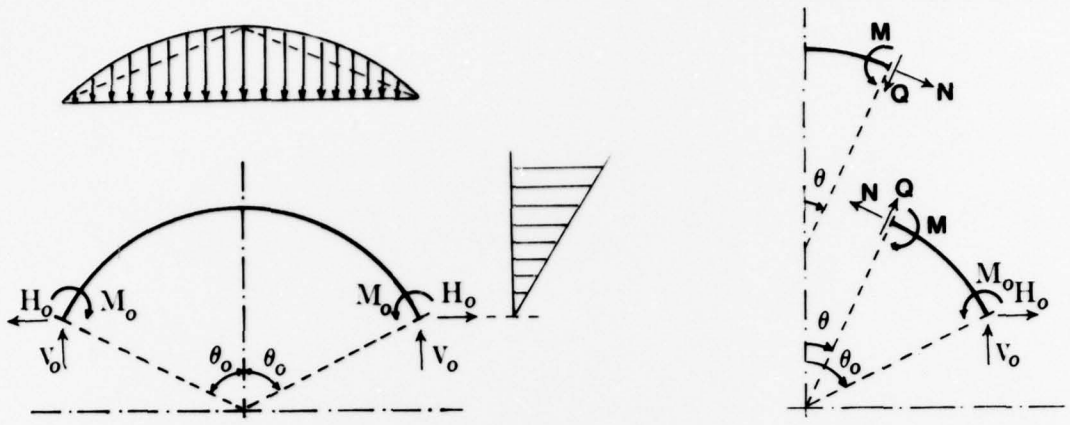

Fig.30 . Sketch of the arch with its load for a given position of the shock wave. The positive directions of the forces at an arbitrary cross section are also shown.

of the arch are given by the shearing force Q , the axial force N and the bending moment M. These quantities have been calculated as functions of θ for each position $\theta = \theta_o$ of the shock wave, and the result is given in the tables in the Appendix. The load function used is given in (4.1) but for comparison also (4.2) has been used. The result can be summed up through Fig.31 where two characteristic situations are exhibited. The distribution of the axial force N, the shearing force Q and the bending moment M over the arch for two different positions, $\theta_o = 54^\circ$ and $\theta_o = 81^\circ$, of the shock wave are shown. The load funtion is given in (4.1) but in the latter case also the results for the load function in (4.2) are shown by dotted lines. It is noticed that the difference between the two load functions is marginal for all quantities except the axial force N. This quantity exhibits a maximum value which does not occur at $\theta = \theta_o$ as Q and M do. Comparing these results to the experimentally obtained yield of the lining (Figs.17 and 18) one finds that the position at which N exhibits ist maximum value corresponds very well to the positions at which yield occurred. Thus one may take this as an encouraging indication that the proposed semi-static approach may render sensible results.

Regarding the yield mechanism for a reinforced concrete structure subjected to the simultaneous action of axial - and shear stress as well as bending stresses no conclusive investigation seems

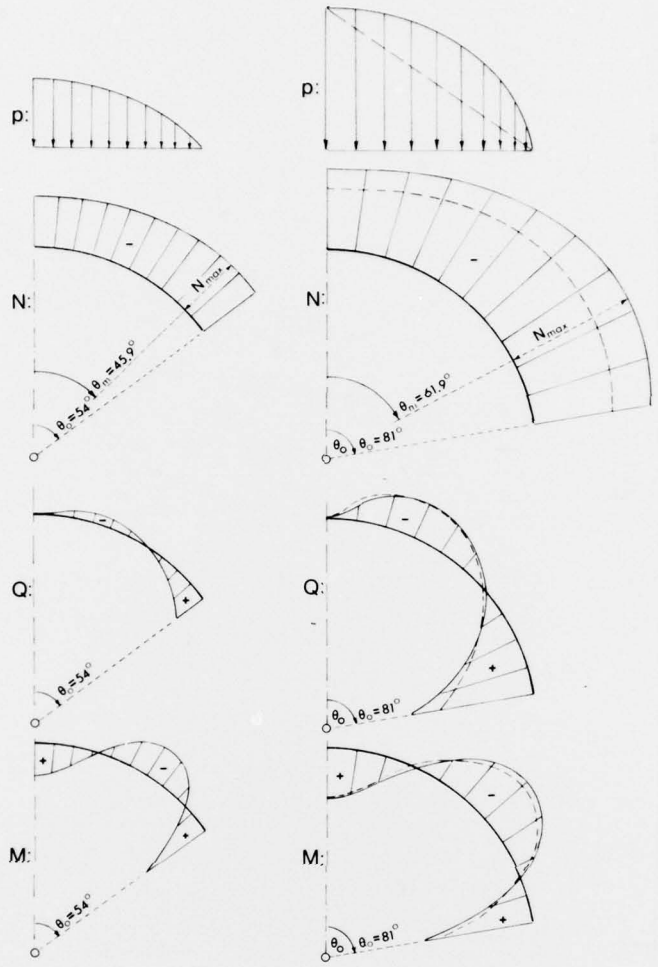

Fig.31. Axial force N, shear force Q and bending moment M in the arch (lining) for two different positions of the shock wave.

to be available in the literature. A recent investigation originating from the activities in the North Sea has been carried out at the Norwegian Institute of Technology (NTH) by LENSCHOW and HOFSØY [2]. The complexity of the situation is perhaps best brought out by a brief account of their results. Fig.32 is a reproduction of Fig.5.4 in [2]. Is shows how the carrying capacity of a reinforced concrete structure depends on the magnitude of axial- and shear forces as well as of bending moments, and indicates the type of failure under different circumstances according to the Norwegian Code NS 3473. It is however clear that the code given this way is valid only for a given relation between the shear force and the

LOAD CAPASITY
According to the Norwegian Code,
NS 3473

Fig 5.4

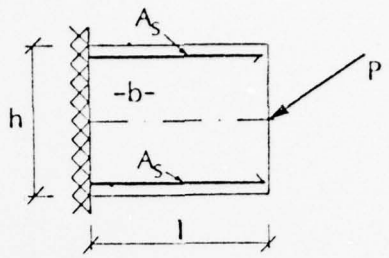

$N_o = f_c bh$

$l/h = 1,2$

$A_s f_s / N_o = 0,1$

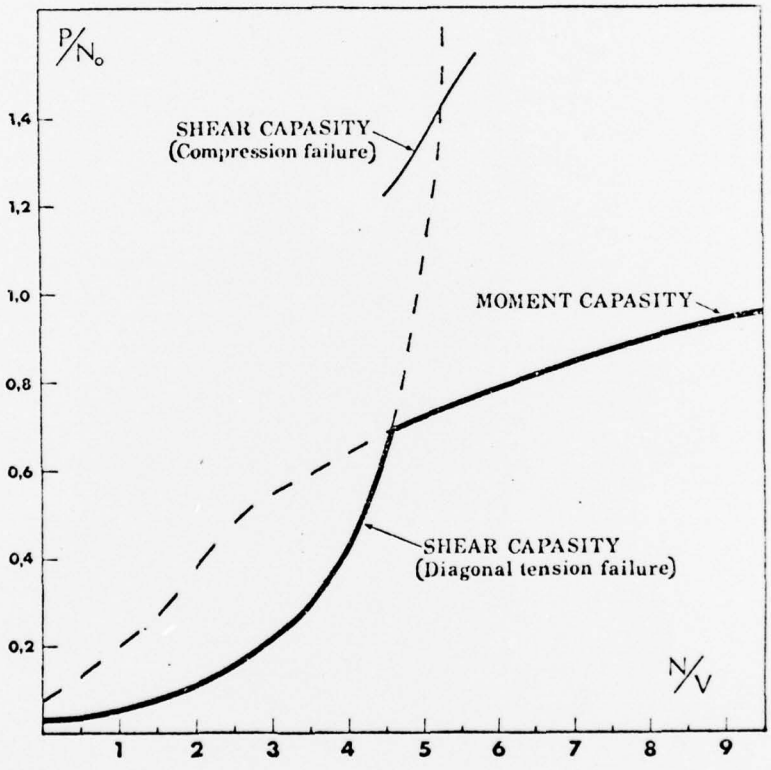

Fig.32 . Reproduction of Fig.5.4 of [2].

bending moment. (The notations used in Fig.32 and later in Fig.33 are explained in the figure. It should be added that f_c and f_s are the design strength of the concrete and the steel respectively. V is the shear stress corresponding to Q in the present notations.)

Fig.33 is a reproduction of Fig.9.8 of [2] which gives a review of the situation. Not only is the Norwegian Code 3473 shown, but also the American Code ACI and the European Code CEB together

Fig 9.8

Analytical model compared with codes
LOAD CAPASITY

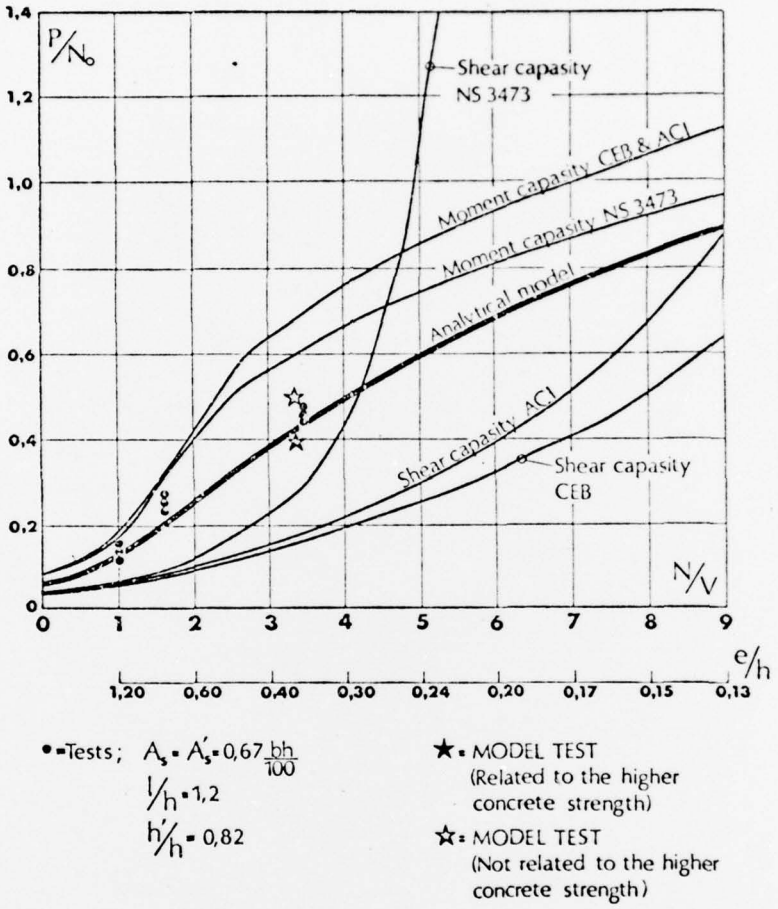

Fig.33 . Reproduction of Fig.9.8 of [2]

with their own results and their analytical model. It seems clear that these results indicate a shear failure at the locations observed if the results from the semi-static calculations are used. Thus, one is again encouraged to try this approach for the determination of the capacity of a lined tunnel to withstand the influence of a shock wave. Again it is stressed that the approach only is aimed at cases where the failure takes place as a "puncture" of the lining during the passage of the first phase of the shock wave.

5. Acknowledgement

The present investigation has been sponsored by the Air Force Cambridge Research Laboratories (AFSC), United States Air Force, under contract No.: F44620-75-C-0029. The United States Government is authorized to reproduce and distribute reprints for governmental purposes notwithstanding any copyright hereon.

The experiments referred to were carried out by A/S NORCONSULT, Oslo and sponsored by the Bundesministerium der Verteidigung, West Germany.

REFERENCES

[1] Leif N. Persen, "Rock Dynamics and Geophysical Exploration", Elsevier Publ. Co., Amsterdam Oxford New York (1975), p.53-67.

[2] R. Lenschow and A. Hofsøy, "Carrying Capacity of the Intersection Between Dome and Cylinder Wall of a reinforced Concrete Structure", A tentative report in two sections, presented at the BOSS '76 Conference ("Behaviour of Offshore Structures") held at The Norwegian Institute of Technology (NTH) August 1976.

APPENDIX

Listing of the static quantities in Fig.30:

N = normalized axial force = $N/p_o R$

Q = normalized shearing force = $Q/p_o R$

M = normalized bending moment = $M/p_o R^2$

H = normalized horizontal force = $H/p_o R$

V = normalized vertical force = $V/p_o R$

Load:

$$p = p_o(\cos\theta - \cos\theta_o)$$

θ	N	Q	M	H	V
5.4	0.2976193	0.0106927	0.0041835	-0.2952921	0.0386537
10.8	0.3043287	0.0194581	0.0027403	-0.2952921	0.0761389
16.2	0.3146305	0.0245367	0.0006319	-0.2952921	0.1113415
21.6	0.3272911	0.0244900	-0.0017233	-0.2952921	0.1432541
27.0	0.3407508	0.0183244	-0.0037916	-0.2952921	0.1710248
32.4	0.3532733	0.0055733	-0.0049699	-0.2952921	0.1939990
37.8	0.3631129	-0.0136671	-0.0046377	-0.2952921	0.2117553
43.2	0.3686870	-0.0387568	-0.0022094	-0.2952921	0.2241311
48.6	0.3687355	-0.0685805	0.0028169	-0.2952921	0.2312394
54.0	0.3624534	-0.1016633	0.0108203	-0.2952921	0.2334748

θ	N	Q	M	H	V
6.3	0.3698939	0.0192214	0.0085370	-0.3655508	0.0596953
12.6	0.3823497	0.0347966	0.0055179	-0.3655508	0.1173656
18.9	0.4012661	0.0434716	0.0011386	-0.3655508	0.1711049
25.2	0.4241081	0.0427303	-0.0036956	-0.3655508	0.2192400
31.5	0.4477584	0.0310547	-0.0078561	-0.3655508	0.2604316
37.8	0.4688888	0.0080665	-0.0101089	-0.3655508	0.2937590
44.1	0.4843575	-0.0254644	-0.0092423	-0.3655508	0.3187839
50.4	0.4915867	-0.0677492	-0.0041872	-0.3655508	0.3355891
56.7	0.4888745	-0.1162320	0.0058842	-0.3655508	0.3447909
63.0	0.4756031	-0.1679353	0.0214916	-0.3655508	0.3475244

θ	N	Q	M	H	V
7.2	0.4343998	0.0320825	0.0158176	-0.4269534	0.0862742
14.4	0.4556313	0.0577563	0.0100741	-0.4269534	0.1692527
21.6	0.4874841	0.0714373	0.0018063	-0.4269534	0.2458756
28.8	0.5251908	0.0690702	-0.0072049	-0.4269534	0.3135393
36.0	0.5630622	0.0486121	-0.0147920	-0.4269534	0.3702877
43.2	0.5952961	0.0102239	-0.0186685	-0.4269534	0.4149611
50.4	0.6167956	-0.0438579	-0.0167018	-0.4269534	0.4472931
57.6	0.6238762	-0.1097486	-0.0071497	-0.4269534	0.4679499
64.8	0.6147549	-0.1825802	0.0111720	-0.4269534	0.4785080
72.0	0.5897480	-0.2573046	0.0388160	-0.4269534	0.4813722

θ	N	Q	M	H	V
8.1	0.4864262	0.0503561	0.0270751	-0.4744782	0.1183918
16.2	0.5202763	0.0901100	0.0169632	-0.4744782	0.2316845
24.3	0.5703848	0.1102571	0.0025257	-0.4744782	0.3352102
32.4	0.6284103	0.1047096	-0.0129945	-0.4744782	0.4251283
40.5	0.6847116	0.0711075	-0.0257519	-0.4744782	0.4987551
48.6	0.7299400	0.0109848	-0.0318445	-0.4744782	0.5548004
56.7	0.7565430	-0.0707326	-0.0278364	-0.4744782	0.5934904
64.8	0.7599111	-0.1667984	-0.0111677	-0.4744782	0.6165688
72.9	0.7389646	-0.2690883	0.0196169	-0.4744782	0.6271743
81.0	0.6960773	-0.3701447	0.0648538	-0.4744782	0.6296040

θ	N	Q	M	H	V
9.0	0.5223397	0.0750055	0.0433399	-0.5041754	0.1557940
18.0	0.5734485	0.1333471	0.0266575	-0.5041754	0.3040259
27.0	0.6480141	0.1612574	0.0030504	-0.5041754	0.4378737
36.0	0.7322989	0.1501685	-0.0219495	-0.5041754	0.5519233
45.0	0.8109627	0.0979510	-0.0419616	-0.5041754	0.6426990
54.0	0.8699423	0.0088550	-0.0507817	-0.5041754	0.7090030
63.0	0.8989571	-0.1078078	-0.0432951	-0.5041754	0.7520329
72.0	0.8931194	-0.2399293	-0.0161033	-0.5041754	0.7752648
81.0	0.8533292	-0.3753059	0.0322469	-0.5041754	0.7841125
90.0	0.7853981	-0.5041754	0.1014541	-0.5041754	0.7853981

θ	N	Q	M	H	V
0.9	0.0065306	0.0000902	0.0000178	-0.0065284	0.0001927
1.8	0.0065372	0.0001763	0.0000157	-0.0065284	0.0003815
2.7	0.0065477	0.0002544	0.0000123	-0.0065284	0.0005625
3.6	0.0065615	0.0003204	0.0000078	-0.0065284	0.0007318
4.5	0.0065778	0.0003704	0.0000024	-0.0065284	0.0008854
5.4	0.0065954	0.0004006	-0.0000037	-0.0065284	0.0010195
6.3	0.0066130	0.0004072	-0.0000101	-0.0065284	0.0011304
7.2	0.0066291	0.0003863	-0.0000164	-0.0065284	0.0012141
8.1	0.0066418	0.0003346	-0.0000221	-0.0065284	0.0012671
9.0	0.0066491	0.0002485	-0.0000267	-0.0065284	0.0012856

θ	N	Q	M	H	V
1.8	0.0411038	0.0002412	0.0000352	-0.0410760	0.0015322
3.6	0.0411853	0.0004467	0.0000242	-0.0410760	0.0030319
5.4	0.0413141	0.0005815	0.0000079	-0.0410760	0.0044669
7.2	0.0414797	0.0006114	-0.0000112	-0.0410760	0.0058053
9.0	0.0416678	0.0005040	-0.0000291	-0.0410760	0.0070160
10.8	0.0418603	0.0002289	-0.0000411	-0.0410760	0.0080687
12.6	0.0420356	-0.0002416	-0.0000414	-0.0410760	0.0089340
14.4	0.0421689	-0.0009323	-0.0000236	-0.0410760	0.0095840
16.2	0.0422327	-0.0018645	0.0000197	-0.0410760	0.0099921
18.0	0.0421969	-0.0030558	0.0000963	-0.0410760	0.0101333

θ	N	Q	M	H	V
2.7	0.0895352	0.0009002	0.0001897	-0.0893934	0.0051169
5.4	0.0899488	0.0016605	0.0001285	-0.0893934	0.0101181
8.1	0.0905995	0.0021455	0.0000375	-0.0893934	0.0148897
10.8	0.0914304	0.0022281	-0.0000674	-0.0893934	0.0193209
13.5	0.0923641	0.0017936	-0.0001644	-0.0893934	0.0233060
16.2	0.0933056	0.0007435	-0.0002267	-0.0893934	0.0267455
18.9	0.0941448	-0.0010013	-0.0002235	-0.0893934	0.0295478
21.6	0.0947600	-0.0034982	-0.0001205	-0.0893934	0.0316310
24.3	0.0950218	-0.0067803	0.0001185	-0.0893934	0.0329233
27.0	0.0947976	-0.0108551	0.0005309	-0.0893934	0.0333652

θ	N	Q	M	H	V
3.6	0.1518059	0.0024234	0.0006644	-0.1513542	0.0119506
7.2	0.1531195	0.0044517	0.0004453	-0.1513542	0.0236076
10.8	0.1551725	0.0057089	0.0001211	-0.1513542	0.0346842
14.4	0.1577672	0.0058567	-0.0002488	-0.1513542	0.0449078
18.0	0.1606413	0.0046107	-0.0005856	-0.1513542	0.0540259
21.6	0.1634806	0.0017554	-0.0007945	-0.1513542	0.0618133
25.2	0.1659352	-0.0028455	-0.0007696	-0.1513542	0.0680771
28.8	0.1676381	-0.0092408	-0.0003992	-0.1513542	0.0726625
32.4	0.1682245	-0.0173891	0.0004284	-0.1513542	0.0754571
36.0	0.1673521	-0.0271588	0.0018199	-0.1513542	0.0763951

θ	N	Q	M	H	V
4.5	0.2230102	0.0054191	0.0018130	-0.2218975	0.0228996
9.0	0.2262330	0.0099095	0.0012021	-0.2218975	0.0451782
13.5	0.2312291	0.0126055	0.0003035	-0.2218975	0.0662365
18.0	0.2374636	0.0127623	-0.0007114	-0.2218975	0.0855179
22.5	0.2442424	0.0098072	-0.0016195	-0.2218975	0.1025282
27.0	0.2507627	0.0033782	-0.0021607	-0.2218975	0.1168539
31.5	0.2561719	-0.0066508	-0.0020557	-0.2218975	0.1281787
36.0	0.2596319	-0.0201620	-0.0010247	-0.2218975	0.1362964
40.5	0.2603837	-0.0368008	0.0011934	-0.2218975	0.1411221
45.0	0.2578087	-0.0560018	0.0048232	-0.2218975	0.1426991